

2mix

**NASA TECHNICAL
MEMORANDUM**

NASA TM X-71936
COPY NO.

NASA TM X-71936

NASA-TM-X-71936) EFFECT OF TRAILING-EDGE
FLAP DEFLECTION ON THE LATERAL AND
LONGITUDINAL-STABILITY CHARACTERISTICS OF
A SUPERSONIC TRANSPORT MODEL HAVING A
(NASA) 55 p HC \$5.75 CSCL 01C

N74-20652
Unclas
G3/02 35319

EFFECT OF TRAILING-EDGE FLAP DEFLECTION ON THE LATERAL
AND LONGITUDINAL-STABILITY CHARACTERISTICS OF A SUPERSONIC
TRANSPORT MODEL HAVING A HIGHLY-SWEPT ARROW WING

By Vernard E. Lockwood

March 19, 1974

This informal documentation medium is used to provide accelerated or special release of technical information to selected users. The contents may not meet NASA formal editing and publication standards, may be revised, or may be incorporated in another publication.

NATIONAL AERONAUTICS AND SPACE ADMINISTRATION
LANGLEY RESEARCH CENTER, HAMPTON, VIRGINIA 23665

1. Report No. NASA TM X-71936	2. Government Accession No.	3. Recipient's Catalog No.	
4. Title and Subtitle Effect of Trailing-Edge Flap Deflection on the Lateral and Longitudinal Stability Characteristics of a Supersonic Transport Model Having a Highly-Swept Arrow Wing		5. Report Date March 19, 1974	6. Performing Organization Code
		8. Performing Organization Report No.	
7. Author(s) Vernard E. Lockwood		10. Work Unit No.	
9. Performing Organization Name and Address NASA Langley Research Center Hampton, Virginia 23665		11. Contract or Grant No.	
		13. Type of Report and Period Covered High-Number TM X	
12. Sponsoring Agency Name and Address National Aeronautics and Space Administration Washington, D. C. 20546		14. Sponsoring Agency Code	
		15. Supplementary Notes Special technical information release, not planned for formal NASA publication.	
16. Abstract A low-speed investigation has been made on a highly-swept wing model having a thickened leading edge to determine the effect of inboard trailing-edge flaps on the characteristics of the model in pitch and sideslip. The tests were made at a Mach number of 0.227 which corresponds to a Reynolds number of about 5.53×10^6 based on the reference chord. The results showed that deflection of the trailing-edge flaps decreased the roll due to sideslip by about 20 percent at a landing lift coefficient of 0.5. The directional-stability parameter, $C_{n\beta}$, was increased by deflection of the flaps and the range of lift coefficients over which it was positive was also increased. The longitudinal stability characteristics of the model without leading-edge devices were improved by increased flap deflection, that is, the pitch-up tendency was delayed to higher lift coefficients. The lift coefficient increment resulting from the first 15° flap deflection compared favorably with that predicted using the method presented in NACA TN 3911.			
17. Key Words (Suggested by Author(s)) (STAR category underlined) <u>Aerodynamics</u> , high sweep, arrow wing, longitudinal stability, dihedral effect, directional stability, trailing-edge flaps		18. Distribution Statement Unclassified-Unlimited	
19. Security Classif. (of this report) Unclassified	20. Security Classif. (of this page) Unclassified	21. No. of Pages 55	22. Price* \$5.75

*Available from { The National Technical Information Service, Springfield, Virginia 22151
{ STIF/NASA Scientific and Technical Information Facility, P.O. Box 33, College Park, MD 20740

NATIONAL AERONAUTICS AND SPACE ADMINISTRATION

EFFECT OF TRAILING-EDGE FLAP DEFLECTION ON THE LATERAL
AND LONGITUDINAL STABILITY CHARACTERISTICS OF A SUPERSONIC
TRANSPORT MODEL HAVING A HIGHLY-SWEPT ARROW WING

By Vernard E. Lockwood
Langley Research Center
Hampton, Virginia

SUMMARY

A low-speed investigation has been made on a highly-swept wing model having a thickened leading edge to determine the effect of inboard trailing-edge flaps on the characteristics of the model in pitch and sideslip. The tests were made at a Mach number of 0.227 which corresponds to a Reynolds number of about 5.53×10^6 based on the reference chord.

The results showed that deflection of the trailing-edge flaps decreased the roll due to sideslip by about 20 percent at a landing lift coefficient of 0.5. The directional-stability parameter, $C_{n\beta}$, was increased by deflection of the flaps and the range of lift coefficients over which it was positive was also increased. The longitudinal stability characteristics of the model without leading-edge devices were improved by increased flap deflection, that is, the pitch-up tendency was delayed to higher lift coefficients. The lift coefficient increment resulting from the first 15° flap deflection compared favorably with that predicted using the method presented in NACA TN 3911.

INTRODUCTION

The National Aeronautics and Space Administration is continuing its research effort toward improving the low-speed characteristics of wings designed for supersonic flight. Considerable research effort has been extended toward improving the longitudinal stability characteristics of highly swept wings as shown in references 1 through 5 but relatively little progress has been made towards reducing the dihedral effect. A recent investigation (reference 6) made on a highly swept wing model has indicated some reductions of dihedral effect are possible through the use of wing tip droop. With a low wing configuration it is difficult to take advantage of this characteristic because ground clearance at the wing tip becomes an important consideration.

Although a small amount of dihedral effect is desirable the amount developed on a highly swept wing such as proposed for a supersonic transport imposes large demands on the lateral control system. Federal air regulations require that an airplane be landed safely in a 30 knot cross wind. This requirement can place a lower limit on the touchdown velocity of the airplane, therefore, it is desirable to keep the dihedral effect as low as possible and to improve the lateral control where practical. Since the roll due to sideslip is a function of angle of attack as well as sideslip angle, any method which tends to increase the loading over the inboard section of the wing should reduce the rolling moments due to sideslip for a given lift coefficient.

The present investigation was made on a highly swept, fixed wing model which has been utilized in several previous investigations.

(See references 1 to 5.) The engine nacelles and two inboard flaps that formed an integral part of the model were removed and two large chord flaps which extended from the fuselage to 43 percent of the semispan were substituted. Lateral and longitudinal characteristics were obtained for several trailing-edge flap deflections over an angle-of-attack range from -2° to 23° at 0° and $\pm 5^\circ$ sideslip. The investigation was made at a Mach number of 0.227 which corresponds to a Reynolds number of 5.53×10^6 based on the reference chord.

SYMBOLS

The data are presented in tabular as well as graphic form. The graphic data are referred to the stability axis system. All data contained herein are based on a different set of reference dimensions than the data of reference 1 through 5; however the moments are referenced to the same longitudinal station (Sta. 66.82). The letters S and B used in conjunction with CRM and CYM of the tabular data refer to the stability and body axis system, respectively. The symbols are defined as follows (with those in parenthesis being used with the tabular data):

C_A (CAF)	axial force coefficient, $\frac{\text{Axial force}}{qS}$
C_D (CD)	drag coefficient, $\frac{\text{Drag}}{qS}$
C_L (CL)	lift coefficient, $\frac{\text{Lift}}{qS}$
C_{ℓ} (CRM)	rolling-moment coefficient, Rolling moment/ qSb
$C_{\ell\beta}$	effective dihedral parameter $\Delta C_{\ell}/\Delta\beta$, per deg

C_m	(CPM)	pitching-moment coefficient, $\frac{\text{Pitching moment}}{qS\bar{c}}$
C_N	(CNF)	normal force coefficient, $\frac{\text{Normal force}}{qS}$
C_n	(CYM)	yawing-moment coefficient, $\frac{\text{Yawing moment}}{qSb}$
$C_{n\beta}$		directional-stability parameter, $\frac{\Delta C_n}{\Delta\beta}$, per deg
C_y	(CSF)	side force coefficient, $\frac{\text{Side force}}{qS}$
$C_{y\beta}$		side-force parameter, $\frac{\Delta C_y}{\Delta\beta}$, per deg
L/D		lift-drag ratio
R		Reynolds number per foot
MACH		Mach number
TTINF		Free-stream total temperature, deg F

Reference Dimensions:

A	aspect ratio, b^2/S , 1.617
b	span 3.975 ft
\bar{c}	chord 3.390 ft
S	area 9.769 sq ft
q (QINF)	free-stream dynamic pressure

Model Component Designations:

B_{13}	116.5 inch body (See figs. 1 and 2)
c	local wing chord

f_2	forebody strake (See fig. 3)
H_4	horizontal tail (See fig. 4)
L_6	leading-edge flap on T_6 (See fig. 5)
T_6	extended wing tip (See figs. 1 and 5)
t_1	trailing-edge flap 1
t_2	trailing-edge flap 2
t_3	trailing-edge flap 3, $\delta = 0^\circ$
t_4	trailing-edge flap 4, $\delta = 5^\circ$
V_8	centerline vertical tail (See fig. 6)
W_3	wing leading edge with .010c radius (See ref. 5)

Angular designations:

α (Alpha)	angle of attack of wing reference line, deg
β (Beta)	angle of sideslip, deg
δ	trailing-edge flap deflection, deg
Δ	incremental value of angle (also coefficient) between $\pm 5^\circ$ sideslip

MODEL AND SUPPORT

A three-view drawing of the model used in the current investigation is shown in figure 1 and a photograph of model and support system is shown in figure 2. The nose section shown in figure 3 is identical to that described in reference 1. An 8.5-inch section was inserted in the body aft of the wing trailing edge giving an overall length to the body, B_{13} , of 116.5 in. The leading edge of the wing was equipped with a fairing, W_3 , which wrapped around the leading edge as illustrated in references 4 and 5. In addition to the increase in radius the fairing effected an increase in camber and a small increase in sweep. The increase in sweep gave a leading-edge panel sweep of 74.24° . The outboard section of the wing, T_6 , which is shown in figure 5 utilized a leading edge flap (L_6) deflected 60° and a trailing-edge flap (t_4) deflected 5° .

The original flaps and nacelles were removed from the wing trailing edge and two flaps t_1 and t_2 as shown in figure 1 were substituted to provide a deflected surface extending from the side of the fuselage to 43 percent of the wing semispan. Flap deflection was accomplished with the aid of separate flaps with deflections of 0° , 5° , 15° , and 30° . The horizontal and vertical tails, H_4 and V_8 , tested with the model are shown in figure 4 and 6, respectively. The model reference dimensions and other geometric characteristics are listed in Table I.

TEST CONDITIONS

The tests were made in slotted test section of the Langley high-speed 7- by 10-foot tunnel at a dynamic pressure of about 74 pounds per square foot which corresponds to a Mach number of about 0.227 and Reynolds number of 5.53×10^6 based on the reference chord. Actual values are tabulated with the data presented in Table II. In order to insure turbulent flow in the model boundary layer, a one-tenth inch wide strip of number 80 carborundum was placed about one inch aft of the leading edge of all model components.

MEASUREMENTS AND CORRECTIONS

The aerodynamic forces and moments were measured by means of a six-component, electrical strain-gage balance housed within the model. The angles of attack were measured directly by means of an accelerometer attached to the model. The angles of sideslip which were preset were corrected for deflection of the balance and sting under load. No corrections were applied to the aerodynamic coefficients for wall constraints because theoretical and experimental studies have indicated that wall corrections to be negligible at the low Mach numbers of this investigation.

PRESENTATION OF DATA

A schedule of runs and a tabulation of the data obtained in the investigation are given in Table II and Table III, respectively. Plotted data showing the lateral stability parameters obtained from $\pm 5^\circ$ of

sideslip are presented in figures 7 to 10. Longitudinal coefficients obtained at zero sideslip are shown in figures 11 to 14 inclusive; data obtained with the outboard flap deflected at 5° sideslip angle are shown in figure 15. (It should be noted that the reference dimensions used herein differ from those used in references 1 through 5, therefore account should be taken of these factors before comparisons are attempted, however, the moment reference is identical to that used in references 1 through 5.)

DISCUSSION

Lateral Characteristics

Effective dihedral. The effect of inboard trailing-edge flap deflection on the lateral characteristics are shown in figures 7 and 8. The data show, as was expected, a lower effective dihedral, C_{l_β} , with flap deflected than with the undeflected flaps. In the range of lift coefficients considered for landing ($C_L \approx 0.5$) C_{l_β} was reduced about 20 percent with the vertical tail off. An additional reduction in C_{l_β} was obtained when the centerline vertical tail, V_8 , was attached to the model.

To provide more information relating to the effect of spanwise loading on the roll due to sideslip the outboard flap, t_4 , was deflected. The results which are presented in figure 9 show as would be expected an increase in dihedral effect for the positively deflected outboard control. These results coupled with those shown in figures 7 and 8 indicate that substantial reductions in C_{l_β} can

be obtained for the landing configuration by increasing the loading over the inboard section of the wing.

Directional stability. Deflection of the trailing-edge flaps generally had a favorable effect on the directional-stability parameter $C_{n_{\beta}}$ as shown in figures 7 and 8. At low lift coefficients ($C_L < 0.5$) deflections of the flap gave positive increments of $C_{n_{\beta}}$ with the vertical tail off. With the vertical tail on deflections of the flap increased the tail contribution of $C_{n_{\beta}}$ resulting in larger values of $C_{n_{\beta}}$ with the 30° flaps than with either the 15° or 0° settings. As with other centerline tail configurations increasing the angle of attack or lift coefficient resulted in losses of $C_{n_{\beta}}$; the model became unstable at C_L 's of 0.75, 0.87, and 0.96 with 0° , 15° , and 30° of flap deflection, respectively. The loss of directional stability probably results from the movement of the vertical tail out of the favorable sidewash field as would be indicated by the variation of $C_{y_{\beta}}$ with C_L . Figure 10 shows that the addition of the forebody strake, f_2 , to the model with the flap deflected 30° tends to alleviate the loss in $C_{n_{\beta}}$ at high-lift coefficients and also reduce the dihedral effect.

Longitudinal Characteristics

Lift. The effect of deflecting trailing-edge flaps, t_1 and t_2 on the characteristics in pitch is presented in figure 11. The 15° flap deflection gave a lift increment of $\Delta C_L = .137$ at 0° angle of attack which agrees favorably with the flap increments predicted using the methods published in reference 7. Considerable separation on

the wing or flap is indicated for 30° flap deflection as the increment in C_L resulting from a flap deflection of 15° to 30° is approximately 70 percent of the value obtained for the first 15° of deflection. Flow separation effects are also noted in the difference in the increments in C_m for the two flap deflections and in the lower values of L/D ratio shown in figure 11.

Longitudinal stability. Data are presented in figures 11 and 12 which show the effect of trailing-edge flap deflection on the pitching-moment coefficients at zero sideslip. It is noted that the curves of C_m against C_L tend to become more linear as the flaps are deflected to greater angles. For example, the pitch-up tendency that begins at a $C_L \approx 0.45$ with the flaps undeflected is delayed to a $C_L \approx 0.9$ with the flaps deflected 30° . (For the same lift conditions the angle of attack for pitchup was increased from 11° to 16° .) It should be noted that the only flow control device other than thickened leading edge was a small leading-edge flap on the tip section of the wing. Had the model been equipped with an inboard leading edge flap the pitch-up tendency would have been materially reduced as illustrated in reference 5.

The contribution of the horizontal tail, H_4 , to the longitudinal stability of the model with the flaps up is shown in figure 13; the data indicate the tail becomes increasingly effective with angle of attack. The use of the strake, f_2 , to improve the directional stability resulted in a small reduction in the longitudinal stability of the model as indicated in figure 14; there was no significant increase in the pitch-up tendency as might be expected. The effect of outboard flap

deflection, t_4 on the longitudinal characteristics ($\beta = 5^\circ$) are shown in figure 15.

Before the advantages of a large span inboard flap can be realized some method for trimming out the pitching moments must be provided. To do so on this configuration with a center of gravity that coincides with the model moment reference and provides static stability to a lift coefficient of about 0.9 would require about 30° of horizontal tail deflection at a lift coefficient of 0.5. This method of trimming would leave little longitudinal control power for maneuvering and would result in lower lift-drag ratios as indicated by the data of figure 12. A solution currently being considered makes use of a stability augmentation system that would require zero or small uploads on the horizontal tail for trim. Combined with a center-of-gravity location with the horizontal-tail loads kept to a minimum, relatively high lift-drag ratios and longitudinal control power can be maintained.

CONCLUDING REMARKS

The results of a low-speed investigation on a highly-swept wing model having thickened leading-edge and inboard trailing-edge flaps are summarized as follows: Deflection of the trailing-edge flaps decreased the dihedral effect, C_{l_β} , about 20 percent at a lift coefficient of 0.5 (landing) with vertical tail off; there was an additional reduction in C_{l_β} when a centerline vertical tail was added. The directional-stability parameter, C_{n_β} , was increased and the range of lift coefficients over which it was positive was also increased.

The longitudinal stability characteristics were improved, that is, the pitch-up tendency was delayed from a lift coefficient of 0.45 with undeflected flaps to about 0.9 with the flaps deflected 30° . The lift coefficient increment obtained from the first 15° flap deflection compared favorably in magnitude with that predicted using the method given in NACA TN 3911; lift increments from 15° to 30° deflection decreased to about 70 percent of the values obtained for the first 15° deflection. The pitching-moment coefficients generated by flap deflection are large; to trim this configuration and maintain static stability through lift coefficients required for approach would require large downloads on the horizontal tail. A stability augmentation system combined with a center-of-gravity location that requires zero or small uploads on the horizontal tail is suggested as method of trimming the configuration which would result in relatively high-lift drag ratios and longitudinal control power.

REFERENCES

1. Lockwood, Vernard E.; and Huffman, Jarrett K.: The Aerodynamic Characteristics of a Fixed Arrow Wing Supersonic Transport Configuration (SCAT 15F-9898). Part I - Stability and Performance Characteristics in the Landing and Take-Off Configuration. NASA LWP-766, June 1969.
2. Lockwood, Vernard E.; and Huffman, Jarrett K.: The Aerodynamic Characteristics of a Fixed Arrow Wing Supersonic Transport Configuration (SCAT 15F-9898). Part IV - Aerodynamic Characteristics in Ground Effect. NASA LWP-828, November 1969.
3. Lockwood, Vernard E.: The Aerodynamic Characteristics of a Fixed Arrow Wing Supersonic Transport Configuration (SCAT 15F-9898). Part IA - Additional Studies of the Stability and Performance Characteristics in the Landing and Take-Off Configuration. NASA LWP-842, January 1970.
4. Lockwood, Vernard E.; and Driver, Cornelius: The Aerodynamic Characteristics of a Fixed Arrow Wing Supersonic Transport Configuration (SCAT 15F-9898). Part IB - Studies of the Low-Speed Stability and Performance Characteristics to 35° Angle of Attack. NASA LWP-899, September 1970.
5. Lockwood, Vernard E.: Effect of Leading-Edge Contour and Vertical-Tail Configuration on the Low-Speed Stability Characteristics of A Supersonic Transport Model Having a Highly-Swept Arrow Wing. NASA LWP-1101, April 1973.
6. Henderson, William P. : Subsonic Aerodynamic Characteristics of a Highly Swept Fixed-Wing Configuration With Variation in Wing-Dihedral Angle. NASA TM X-2261, April 1971.
7. Lowry, John G.; and Polhamus, Edward C.: A Method For Predicting Lift Increments Due to Flap Deflection at Low Angles of Attack in Incompressible Flow. NACA TN 3911, 1957.

TABLE I.- DIMENSIONAL CHARACTERISTICS OF MODEL

Reference Dimensions:

Area, sq ft	9.769
Chord, ft	3.389
Span, ft	3.975
Aspect ratio	1.617
Sweep of leading edge	
Main wing, deg	74.24
Tip, deg	60.0

Fuselage

Length, ft	9.708
------------	-------

Horizontal Tail, H_4

Root chord, ft	0.853
Tip chord, ft	0.310
Panel span, ft	0.372
Panel area, sq ft	0.2029
Panel aspect ratio	0.6808
Overall span, ft	0.743
Sweep	
Leading edge	60.0
Trailing edge	-2.0
Dihedral angle, deg	-15.0
Airfoil section, circular arc	
Thickness ratio	
tip	0.075
root	0.040

Vertical Tail, V_8

Root chord, ft	1.333
Tip chord, ft	0.167
Span, ft	0.667
Area, sq ft	0.500
Aspect ratio	0.890
Thickness, ft	0.021
Leading edge sweep, deg	63.4
Trailing edge sweep, deg	4.36

TABLE I.- Concluded

Flaps (trailing edge)

t_1		
Chord, ft.		0.388
Span,		0.308
Area (panel) sq ft		0.1196
Sweep of trailing edge, deg		0.0
t_2		
Chord, ft		
inboard, ft		0.388
outboard, in.		0.564
Span, in.		0.417
Area (panel) sq ft		0.198
Sweep of trailing edge, deg		23°
t_3 (undeflected)		
t_4		
Chord,		0.130
Span,		0.568
Area, sq ft		0.0738
Sweep of trailing edge, deg		36.6

TABLE II.- 949 TEST PROGRAM

RUN	Angular deflections, deg					Model Configuration		
	t_1	t_2	t_3	t_4	i_t	β	V_8	f_2
3	0	0	0	5	Off	0	On	Off
5	0	0			0			
6	5	5						
7	30	30						
9	15	15			-10			
10					0			
15					-10	-5		
16	30	30						
17	0	0						
18							Off	
19				30				
20	15	15		5				
21	30	30						
23	15	15				5		
24	30	30						
25	0	0						
26				30				
27				5			On	
28	15	15						
29	30	30						
30								On
31						0		On
32						0		Off

Table with columns: POINT, MACH, QINF LBS/ SQ FT, BETA DEG, ALPHA DEG, CL, CD, CPM, CRM,S, CYM,S, CSF, L/D, R MILLION PER FOOT. Includes sub-headers: HIGH SPEED TUNNEL, STANDARD STING, TEST 949, RUN 15, BALANCE 731-B, 08/09/72, STABILITY AXIS COEFFICIENTS.

Table with columns: POINT, MACH, QINF LBS/ SQ FT, BETA DEG, ALPHA DEG, CNF, CAF, CPM, CRM,B, CYM,B, CSF, TTINF DEG F. Includes sub-headers: STABILITY AXIS COEFFICIENTS, BODY AXIS COEFFICIENTS.

Table with columns: POINT, MACH, QINF LBS/ SQ FT, BETA DEG, ALPHA DEG, CL, CD, CPM, CRM,S, CYM,S, CSF, L/D, R MILLION PER FOOT. Includes sub-headers: HIGH SPEED TUNNEL, STANDARD STING, TEST 949, RUN 16, BALANCE 731-B, 08/09/72, STABILITY AXIS COEFFICIENTS.

Table with columns: POINT, MACH, QINF LBS/ SQ FT, BETA DEG, ALPHA DEG, CNF, CAF, CPM, CRM,B, CYM,B, CSF, TTINF DEG F. Includes sub-headers: STABILITY AXIS COEFFICIENTS, BODY AXIS COEFFICIENTS.

HIGH SPEED TUNNEL		STANDARD STING			TEST 949	RUN 32	BALANCE 731-B			08/09/72			
POINT	MACH	QINF IRS/ SQ FT	BETA DEG	ALPHA DEG	CL	CO	STABILITY AXIS COEFFICIENTS					1/D	R MILLION PER FOOT
							CPM	CRM,S	CYM,S	CSF			
715	.227	73.692	-.02	.01	.2541	.05485	-.0217	-.0001	.0013	-.0013	4.633	1.601	
716	.229	74.655	-.02	-2.26	.1869	.04981	-.0152	.0003	.0018	-.0021	3.751	1.610	
717	.230	75.329	-.02	-.00	.2549	.05531	-.0216	-.0001	.0013	-.0014	4.610	1.616	
718	.229	74.366	-.01	1.97	.3075	.06057	-.0274	.0021	.0006	-.0006	5.076	1.606	
719	.227	73.307	-.00	2.99	.3510	.06746	-.0323	.0001	-.0001	.0006	5.203	1.594	
720	.226	72.922	.00	4.04	.3864	.07363	-.0367	-.0031	-.0006	.0021	5.248	1.589	
721	.227	73.692	.01	5.15	.4284	.08335	-.0422	-.0003	-.0018	.0040	5.139	1.597	
722	.227	73.596	.02	6.00	.4612	.09175	-.0466	-.0001	-.0028	.0062	5.027	1.595	
723	.226	73.018	.02	7.00	.4956	.10266	-.0504	-.0002	-.0027	.0058	4.828	1.589	
724	.227	73.403	.02	8.03	.5356	.11638	-.0530	.0000	-.0021	.0044	4.602	1.593	
725	.227	73.403	.01	8.99	.5708	.13091	-.0538	.0007	-.0017	.0034	4.360	1.592	
726	.226	72.921	.01	9.99	.6173	.14950	-.0567	.0011	-.0010	.0024	4.129	1.587	
727	.226	72.825	.01	12.30	.7407	.20287	-.0703	.0008	-.0008	.0001	3.651	1.585	
728	.226	72.536	.04	14.08	.8268	.24839	-.0789	.0009	-.0018	-.0025	3.329	1.582	
729	.227	73.403	.13	16.04	.9228	.30694	-.0850	-.0001	-.0054	-.0077	3.007	1.590	
730	.226	72.729	.14	18.00	1.0079	.37065	-.0810	-.0019	-.0063	-.0057	2.719	1.582	
731	.225	72.343	-.05	19.96	1.0843	.43873	-.0771	-.0027	.0034	.0035	2.471	1.577	
732	.226	72.632	-.09	22.02	1.1912	.53001	-.0726	-.0010	.0067	-.0018	2.248	1.579	
733	.226	72.439	-.02	22.95	1.2103	.56271	-.0664	-.0021	.0042	-.0064	2.152	1.576	

POINT	MACH	QINF IRS/ SQ FT	BETA DEG	ALPHA DEG	CNF	CAF	BODY AXIS COEFFICIENTS					TTIME DEG F
							CPM	CPM,B	CYM,B	CSF		
715	.227	73.692	-.02	.01	.2541	.05481	-.0217	-.0001	.0013	-.0013	53.0	
716	.229	74.655	-.02	-2.26	.1840	.05716	-.0152	.0004	.0017	-.0021	53.3	
717	.230	75.329	-.02	-.00	.2549	.05533	-.0216	-.0001	.0013	-.0014	53.5	
718	.229	74.366	-.01	1.97	.3094	.04997	-.0274	.0001	.0006	-.0006	53.6	
719	.227	73.307	-.00	2.99	.3540	.04906	-.0323	.0001	-.0001	.0006	53.7	
720	.226	72.922	.00	4.04	.3906	.04622	-.0367	-.0001	-.0006	.0021	53.8	
721	.227	73.692	.01	5.15	.4341	.04455	-.0422	-.0001	-.0018	.0040	53.9	
722	.227	73.596	.02	6.00	.4683	.04302	-.0466	.0002	-.0028	.0062	54.0	
723	.226	73.018	.02	7.00	.5044	.04154	-.0504	.0002	-.0027	.0058	54.1	
724	.227	73.403	.02	8.03	.5466	.04046	-.0530	.0003	-.0021	.0044	54.2	
725	.227	73.403	.01	8.99	.5842	.04013	-.0538	.0010	-.0016	.0034	54.3	
726	.226	72.921	.01	9.99	.6338	.04013	-.0567	.0013	-.0009	.0024	54.4	
727	.226	72.825	.01	12.30	.7669	.04041	-.0703	.0010	-.0006	.0001	54.4	
728	.226	72.536	.04	14.08	.8624	.03976	-.0789	.0013	-.0015	-.0025	54.6	
729	.227	73.403	.13	16.04	.9717	.03995	-.0850	.0014	-.0057	-.0077	54.9	
730	.226	72.729	.14	18.00	1.0731	.04103	-.0810	.0002	-.0066	-.0057	55.1	
731	.225	72.343	-.05	19.96	1.1689	.04218	-.0771	-.0037	.0022	-.0035	55.2	
732	.226	72.632	-.09	22.02	1.3030	.04463	-.0726	-.0034	.0058	-.0018	55.5	
733	.226	72.439	-.02	22.95	1.3337	.04598	-.0664	-.0036	.0030	-.0064	55.6	

Reference dimensions

Area 9.769 sqft
 Spon 3.975 ft
 Chord 3.390 ft

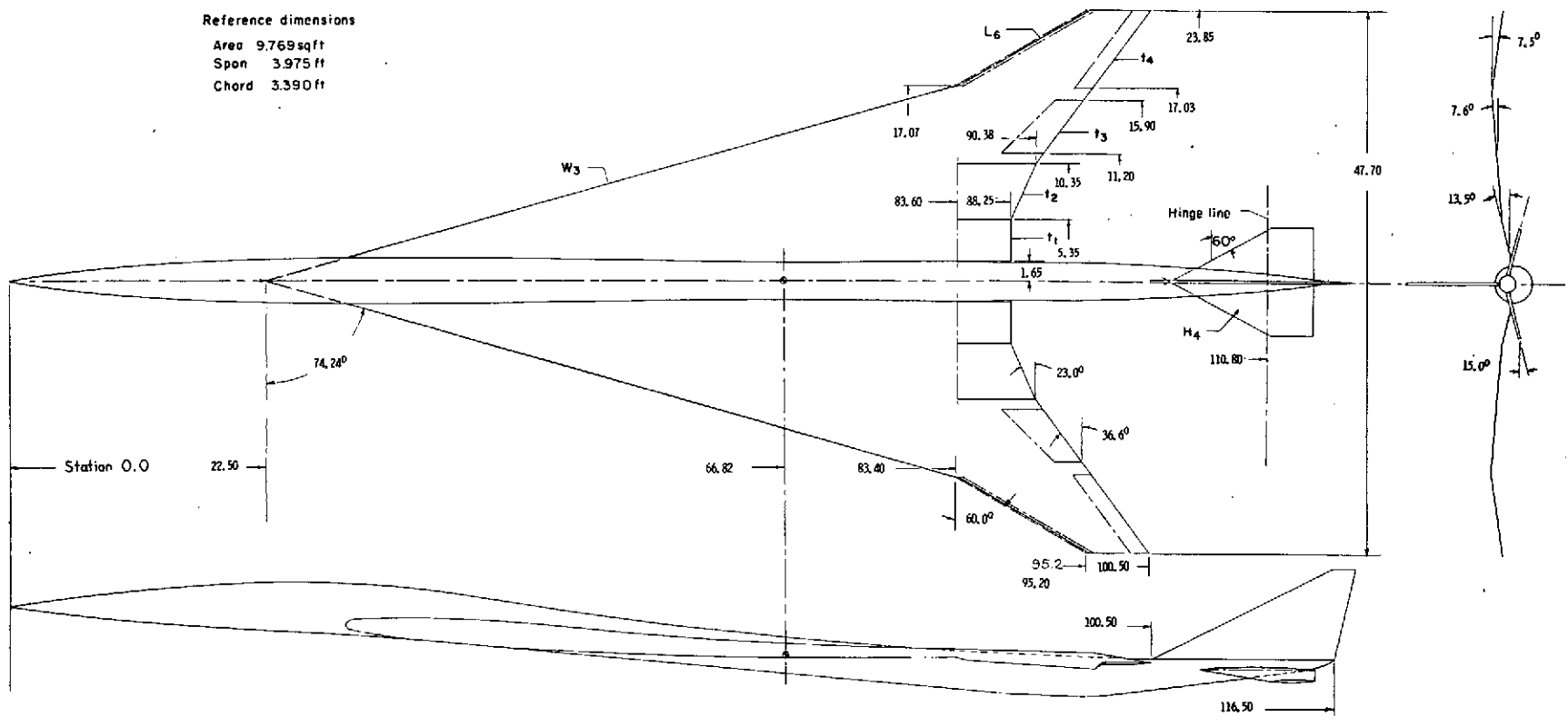


Figure 1.- Three-view drawing of model.

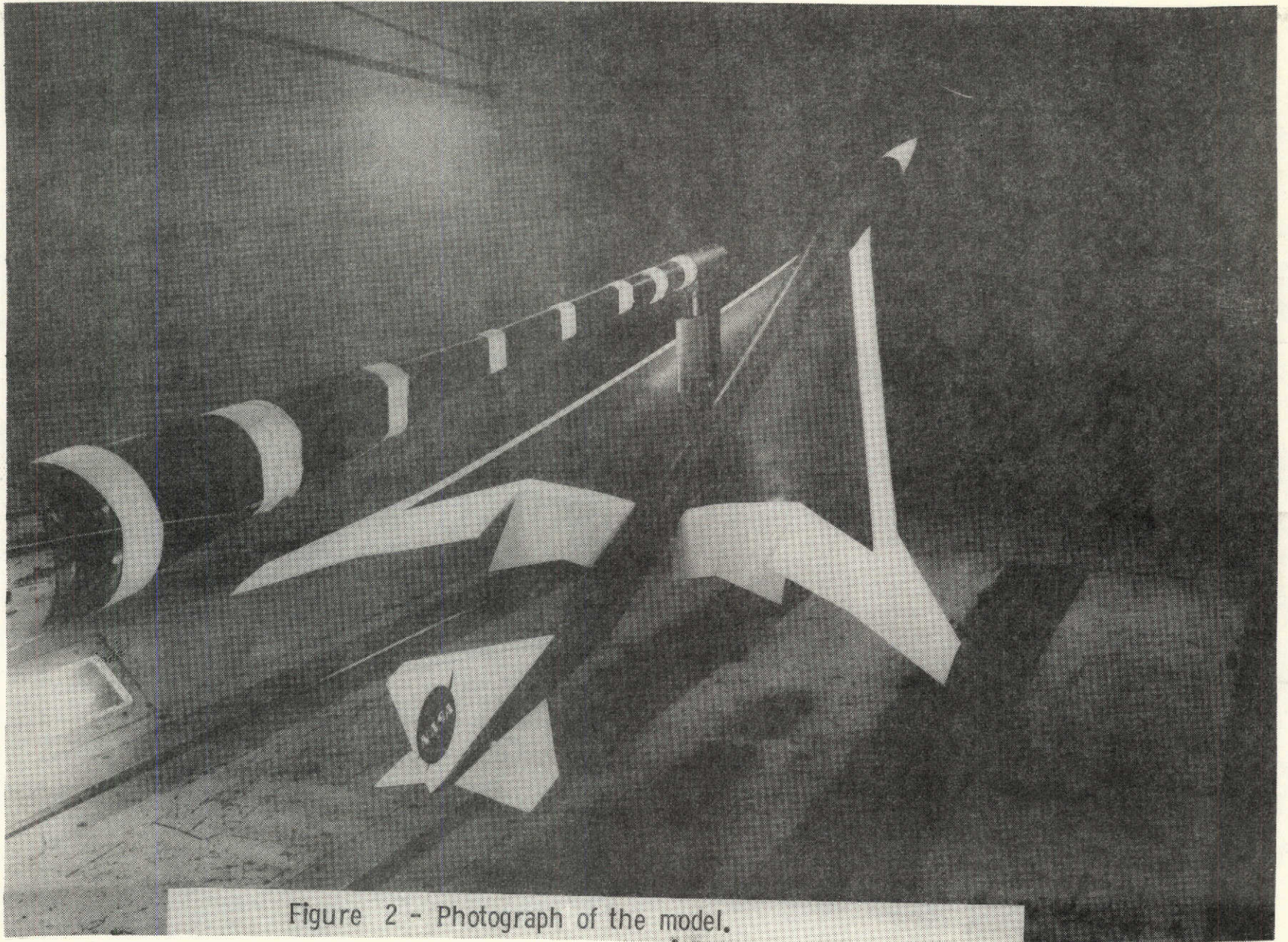


Figure 2 - Photograph of the model.

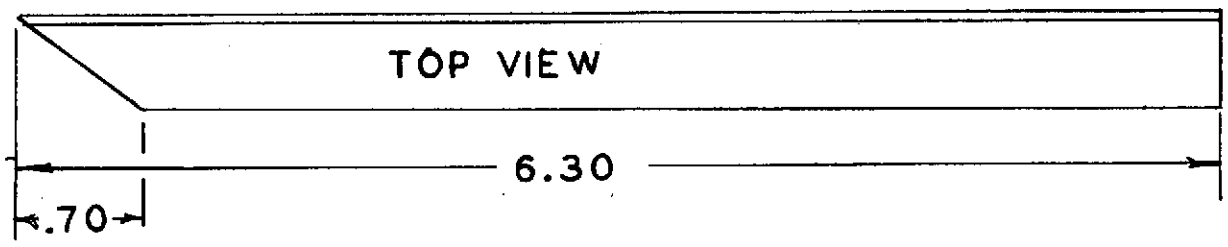
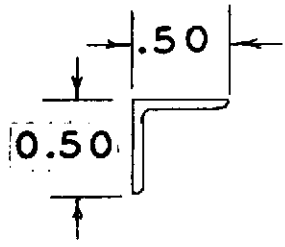
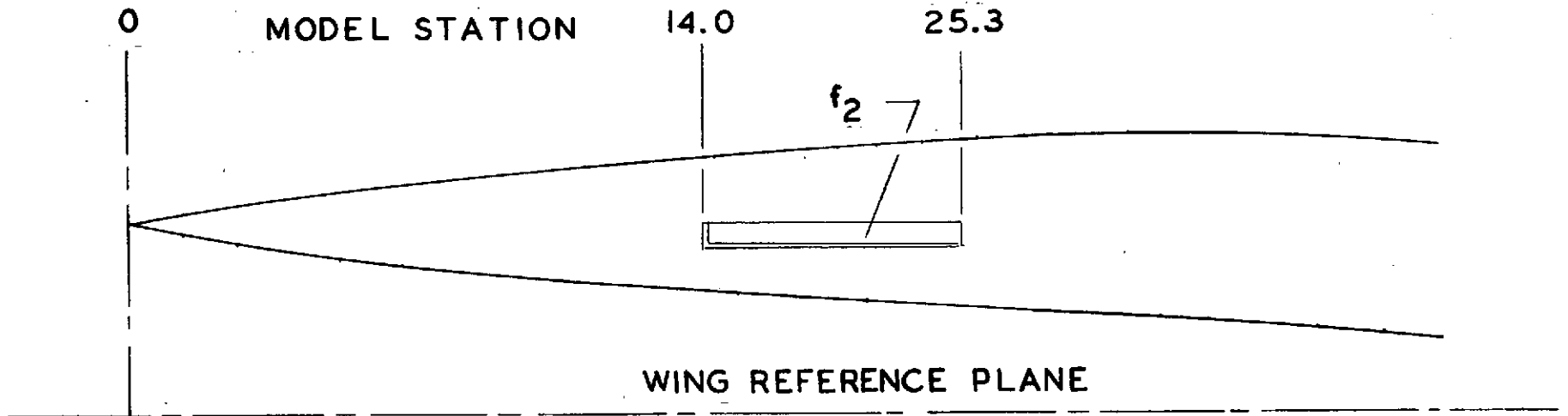


Figure 3 .- Drawing of fuselage nose with strake, f_2 , attached.

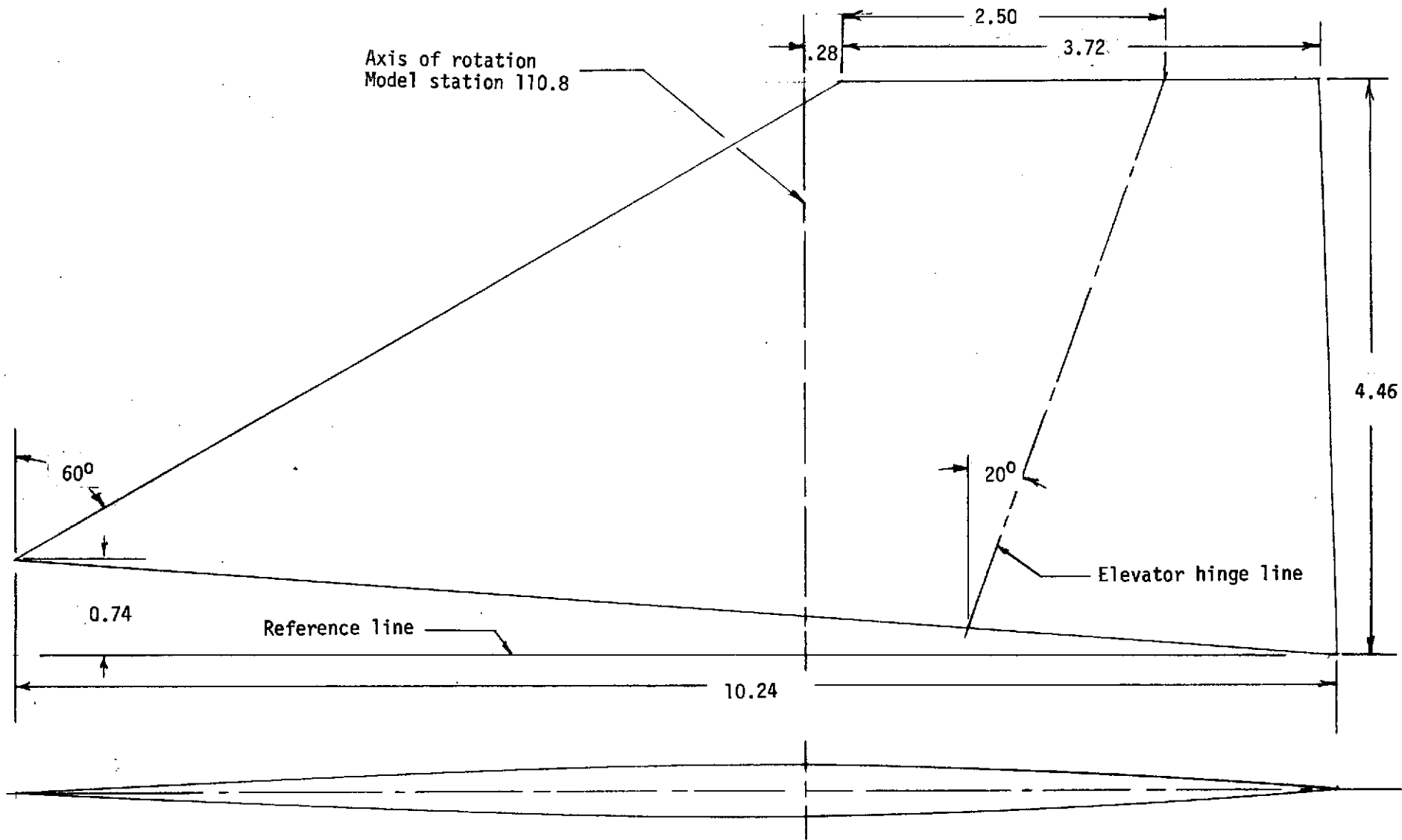


Figure 4.- Drawing of the horizontal tail, H_4 .

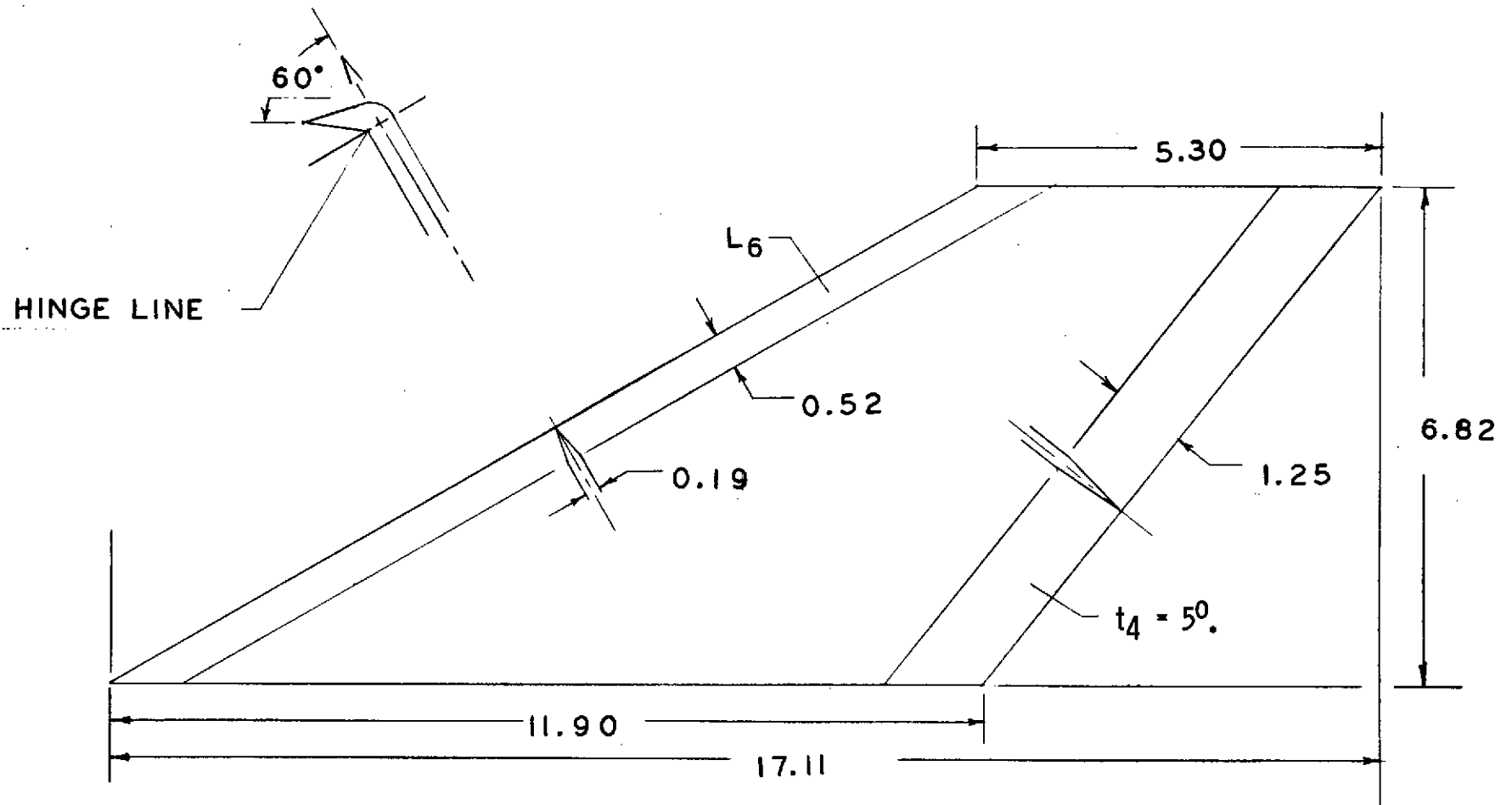


Figure 5.- Details of the extended wing tip, T6.

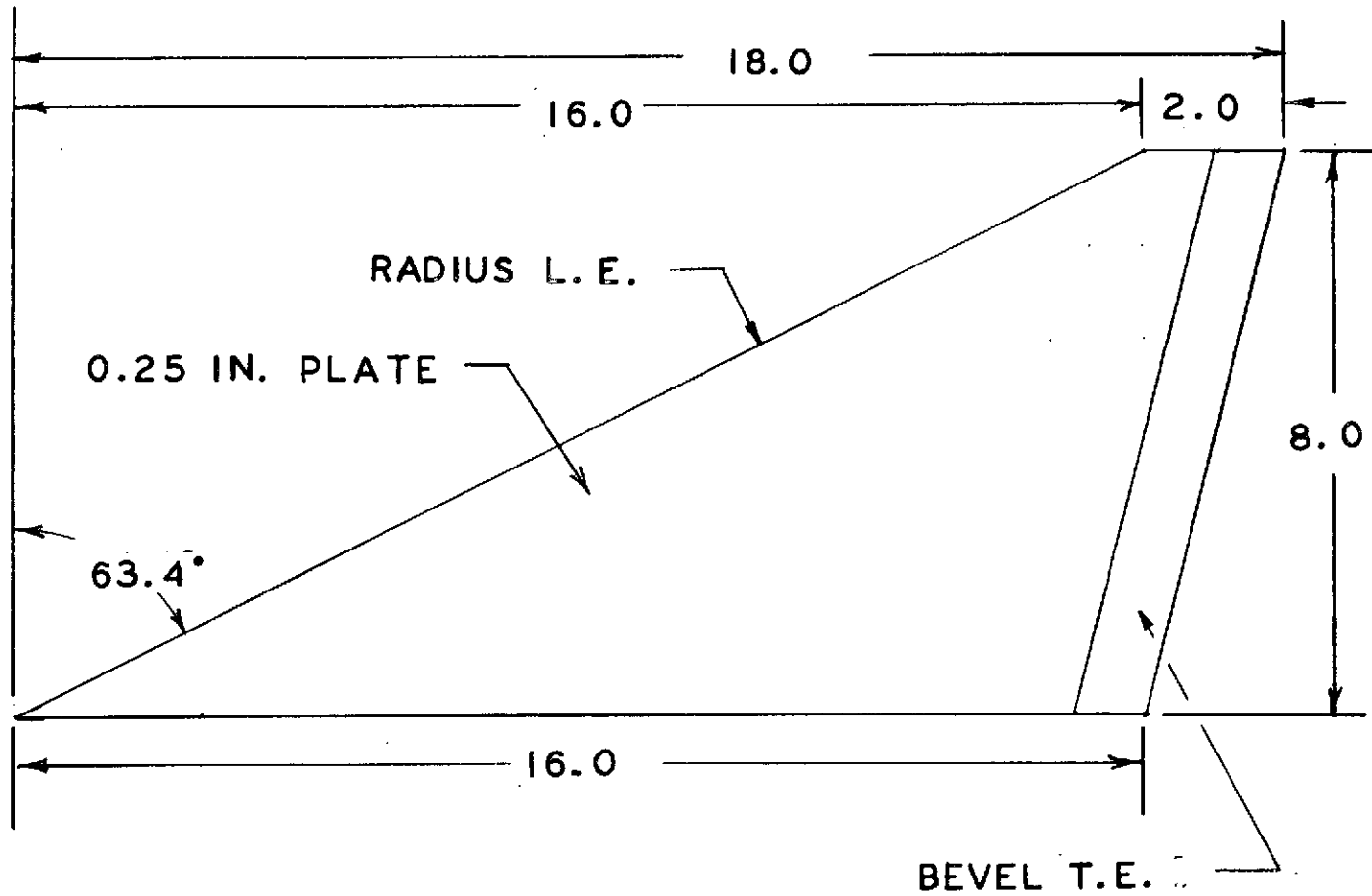
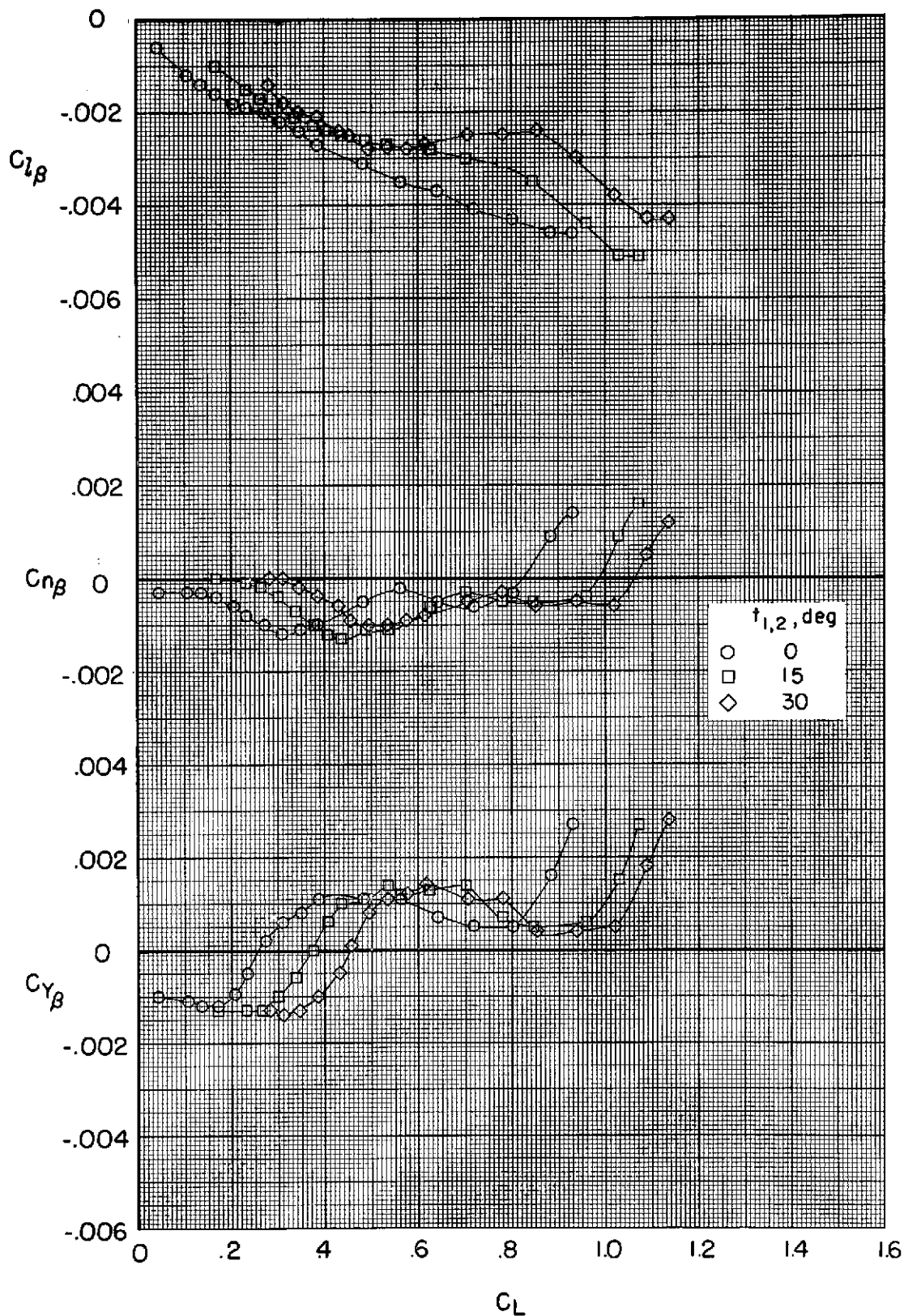
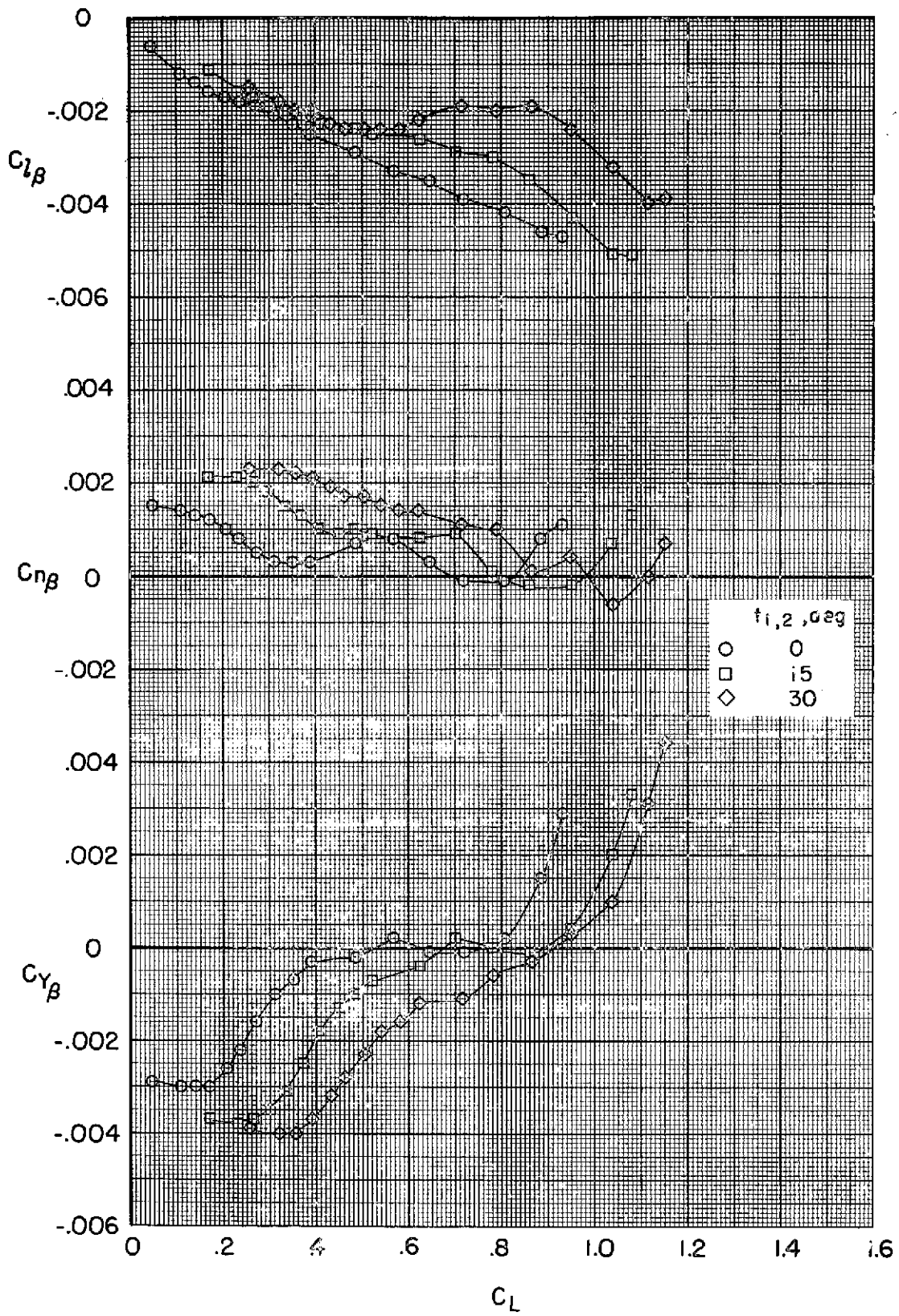


Figure 6.- Details of the vertical tail, V₈.



(a) Vertical tail off
 Figure 7.- Effect of trailing-edge flap deflection on the lateral-directional stability parameters. $i_t = -10^\circ$, $t_3 = 0^\circ$, $t_4 = 5^\circ$.



(b) Vertical tail on
Figure 7.- Concluded.

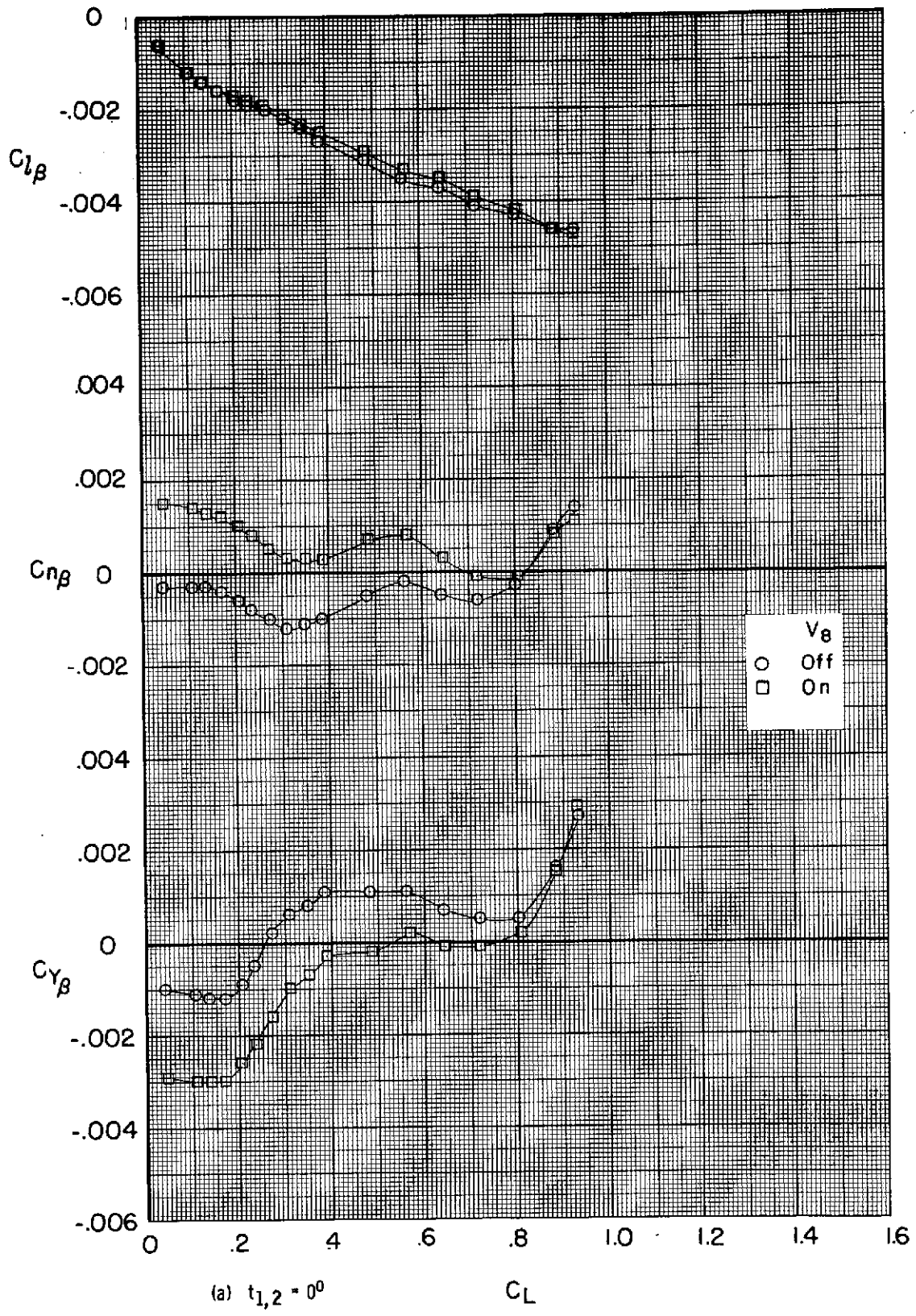
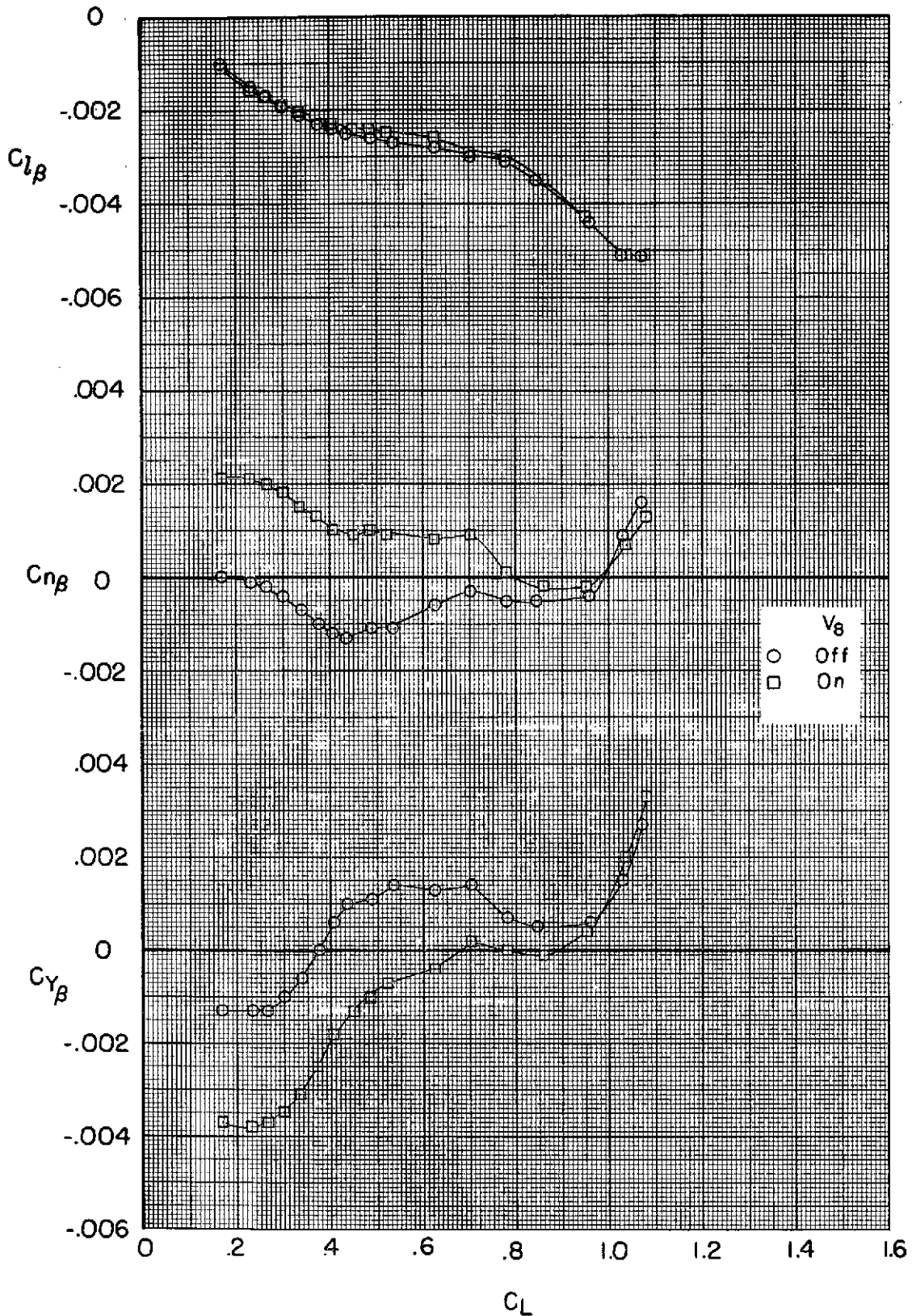
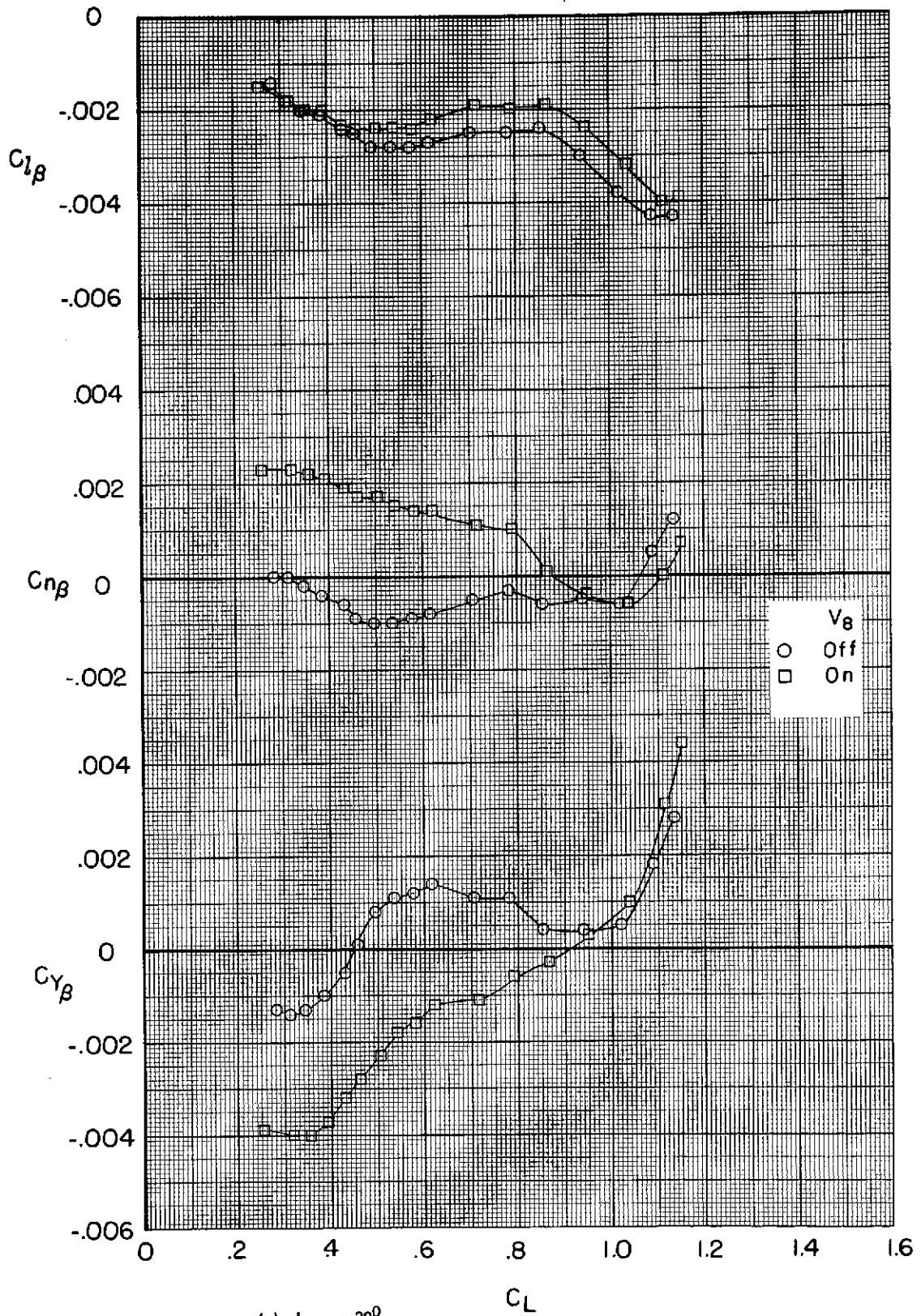


Figure 8.- Effect of the vertical tail on the lateral-directional stability parameters.
 $t_1 = -10^\circ$, $t_3 = 0^\circ$, $t_4 = 5^\circ$.



(b) $t_{1,2} = 15^\circ$
 Figure 8.- Continued.



(c) $t_{1,2} = 30^\circ$
 Figure 8. - Concluded.

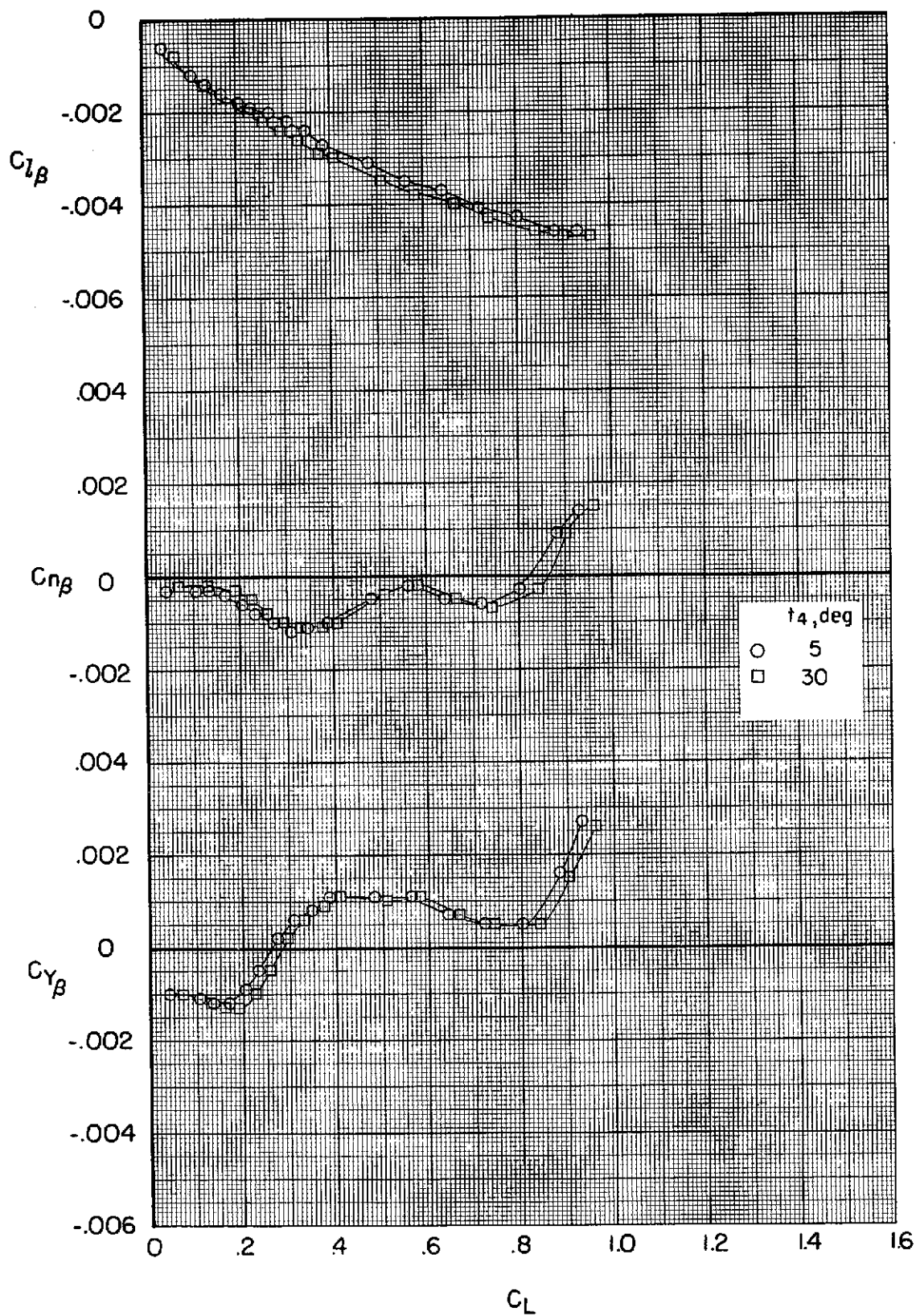


Figure 9 .- Effect of trailing-edge flap deflection, t_4 , on the lateral-directional stability parameters. $t_1 = -10^\circ$, $t_{1,2} = 0^\circ$, $t_3 = 0^\circ$, V_{off} .

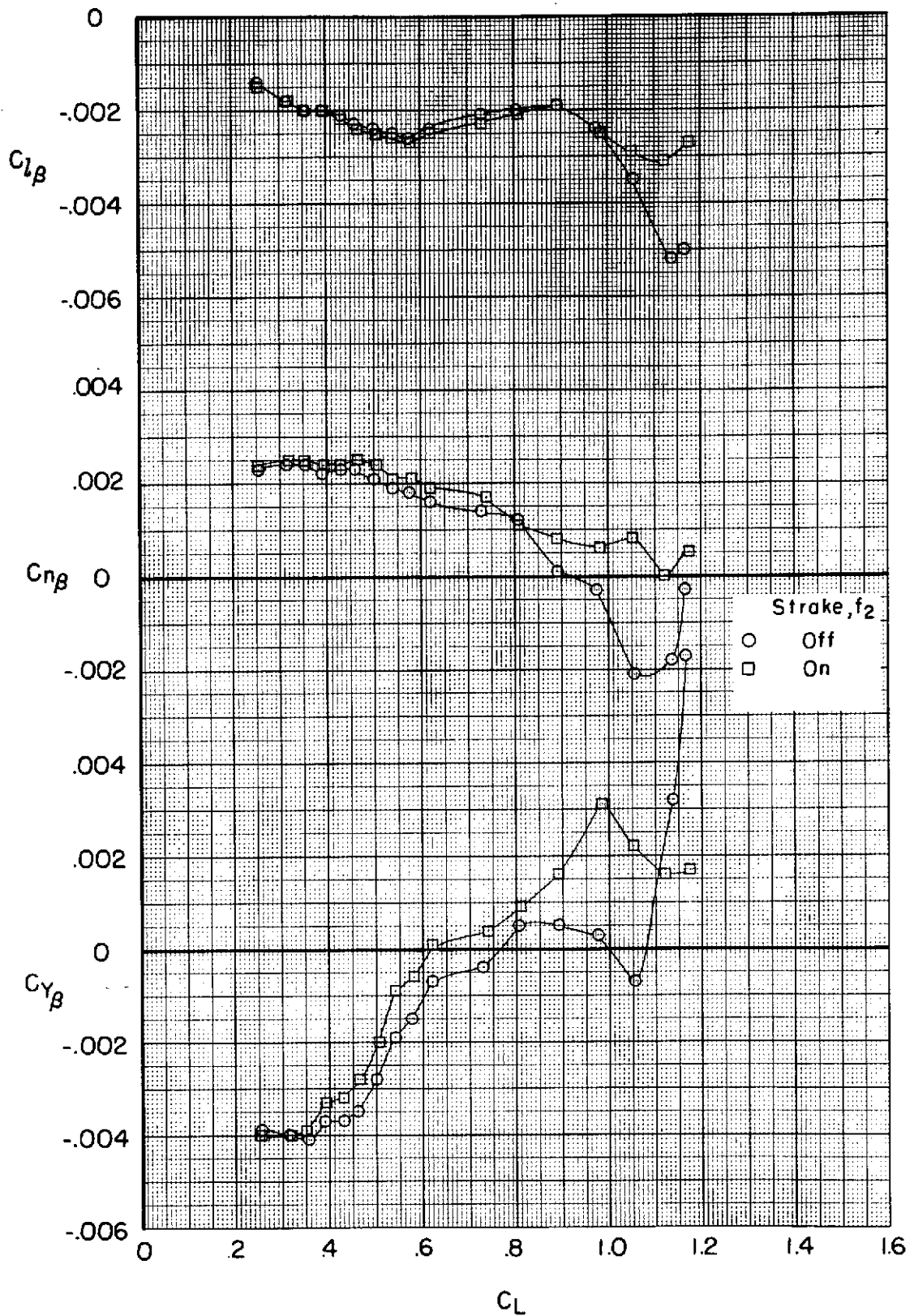


Figure 10 .- Effect of the strake, f_2 , on the lateral-directional stability parameters. $i_t = -10^\circ$, $t_{1,2} = 30^\circ$, $t_3 = 0^\circ$, $t_4 = 5^\circ$, V_{on} .

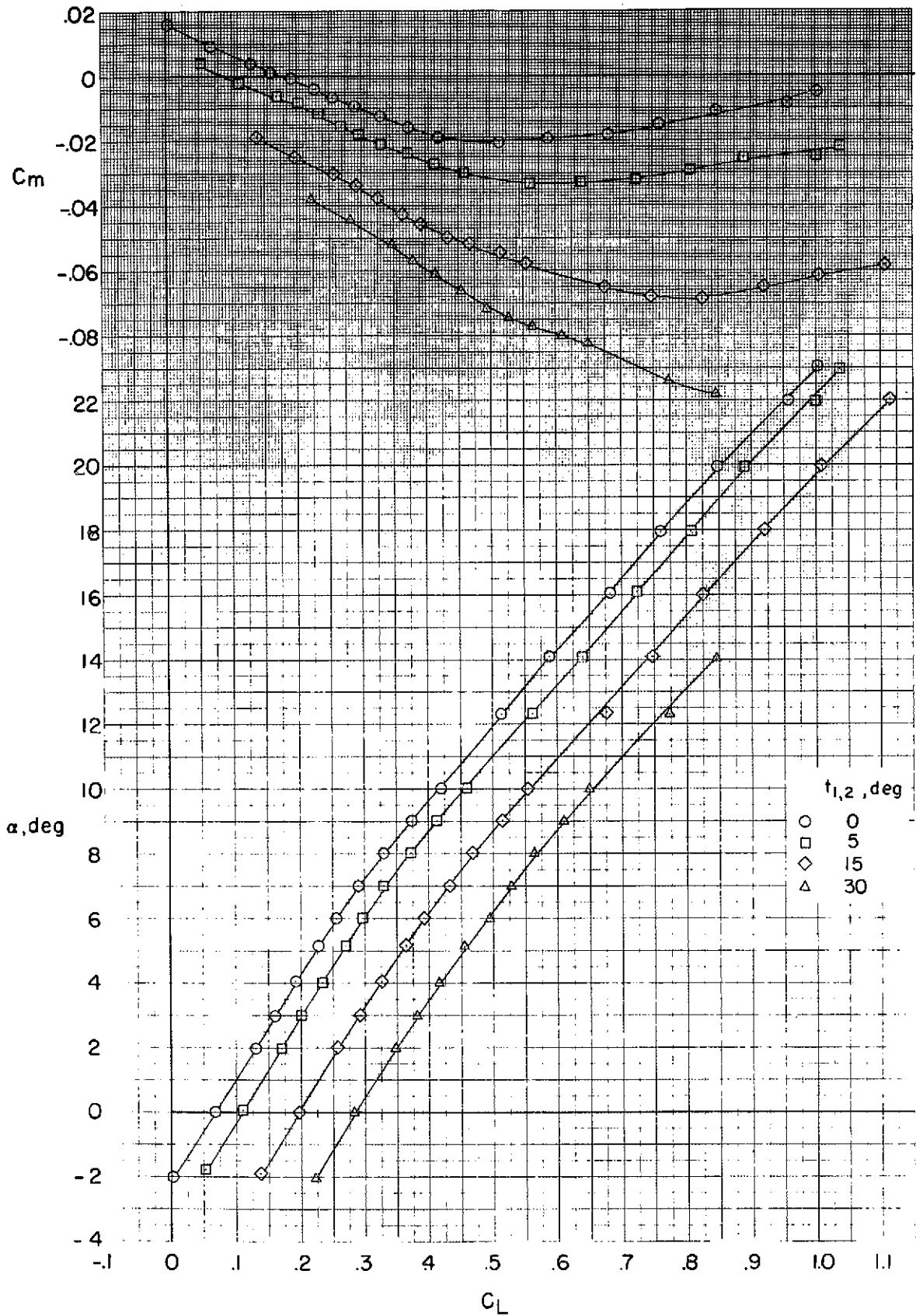


Figure 11.- Effect of trailing-edge flap deflection on the longitudinal characteristics.
 $t_3 = 0^\circ$, $t_4 = 5^\circ$, $t_t = 0^\circ$, V_{0n} .

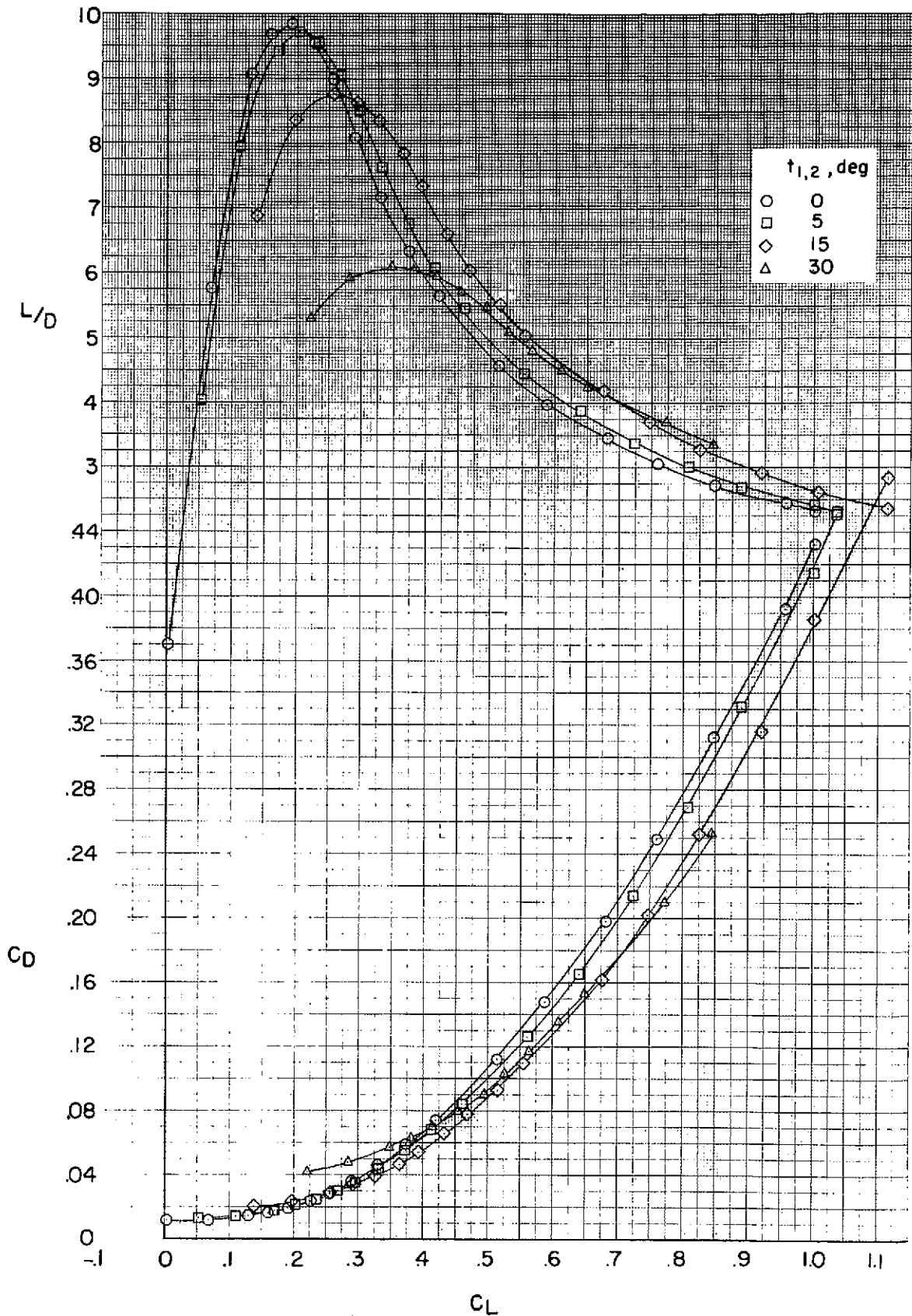
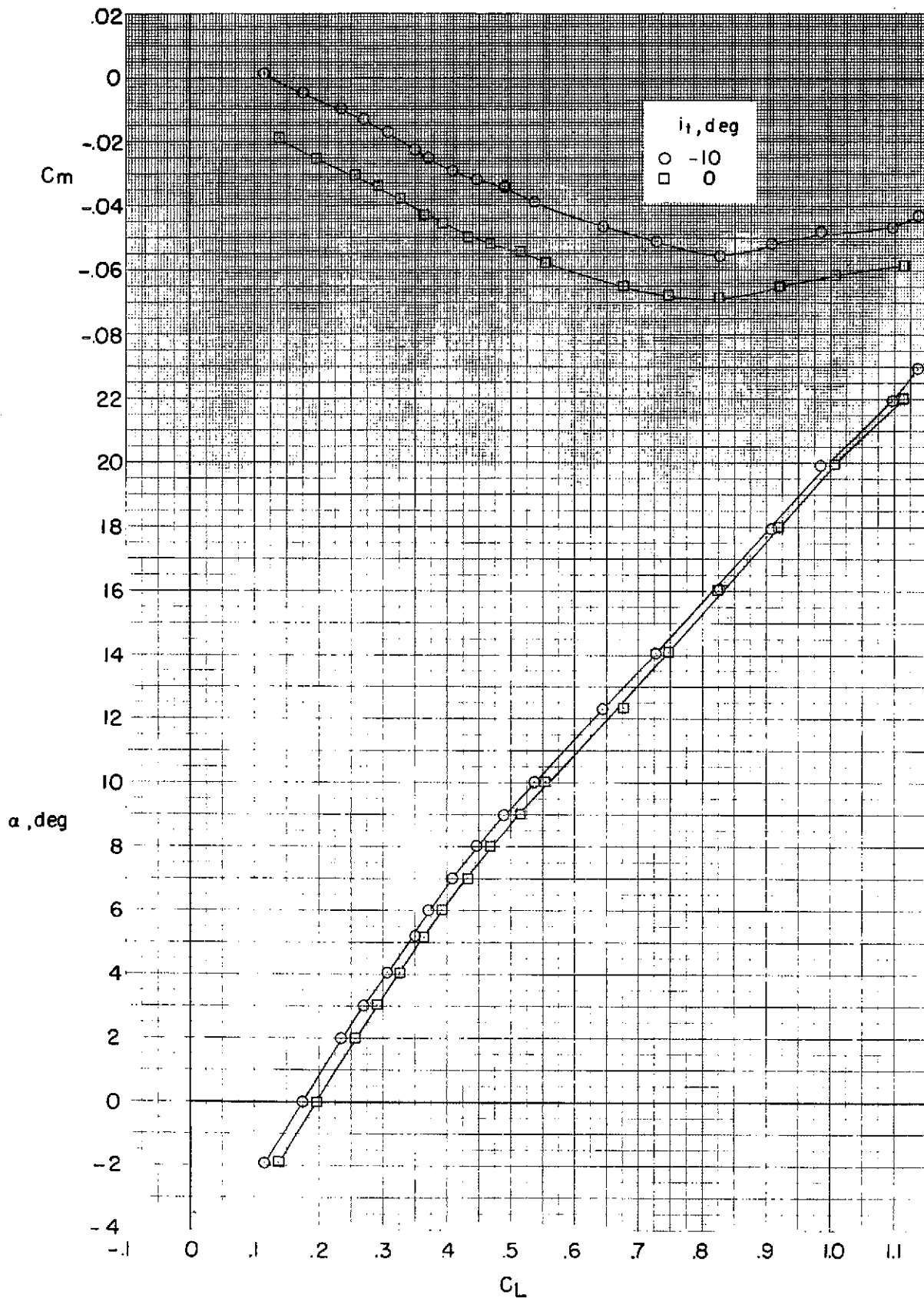
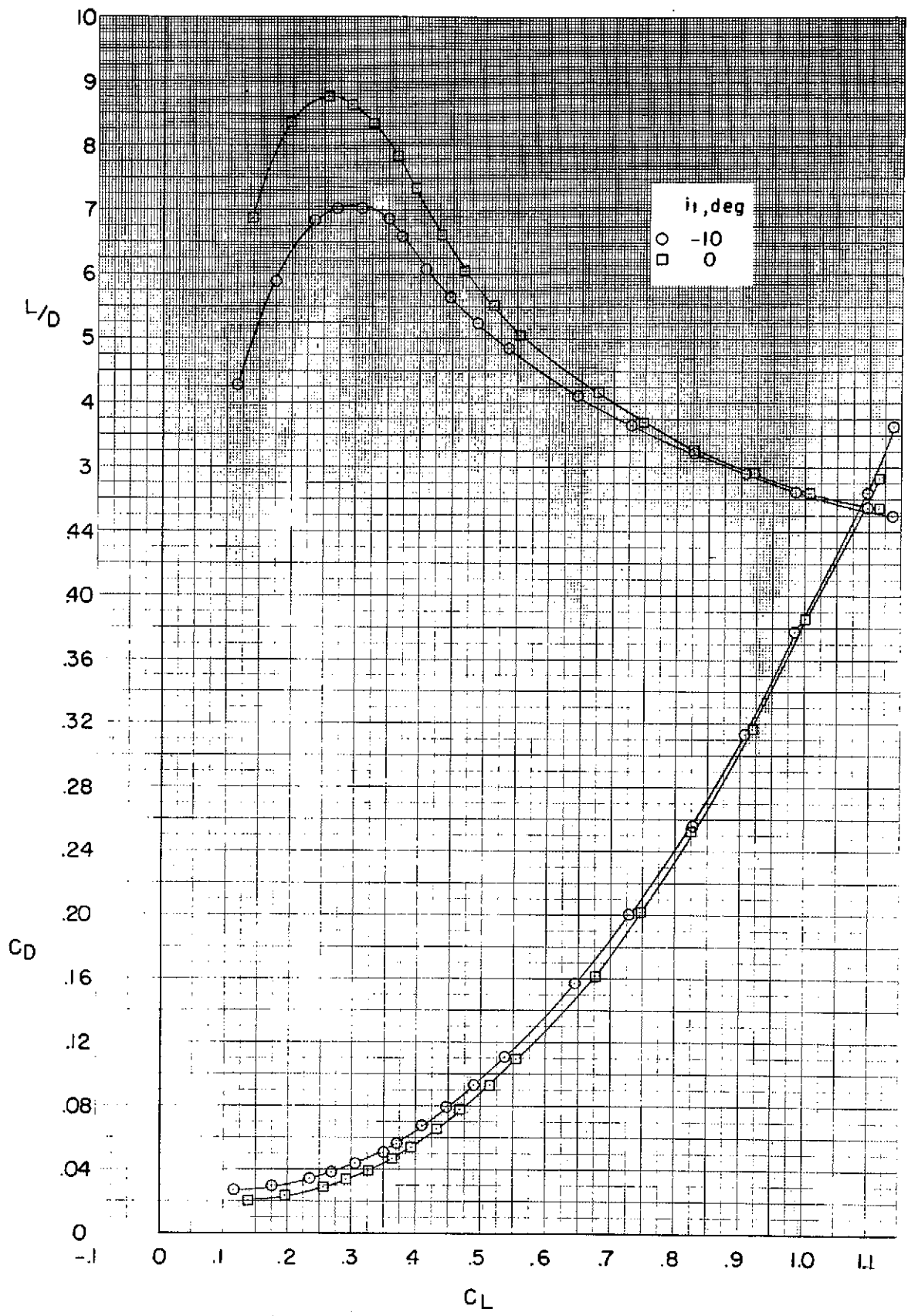


Figure 11.- Concluded.

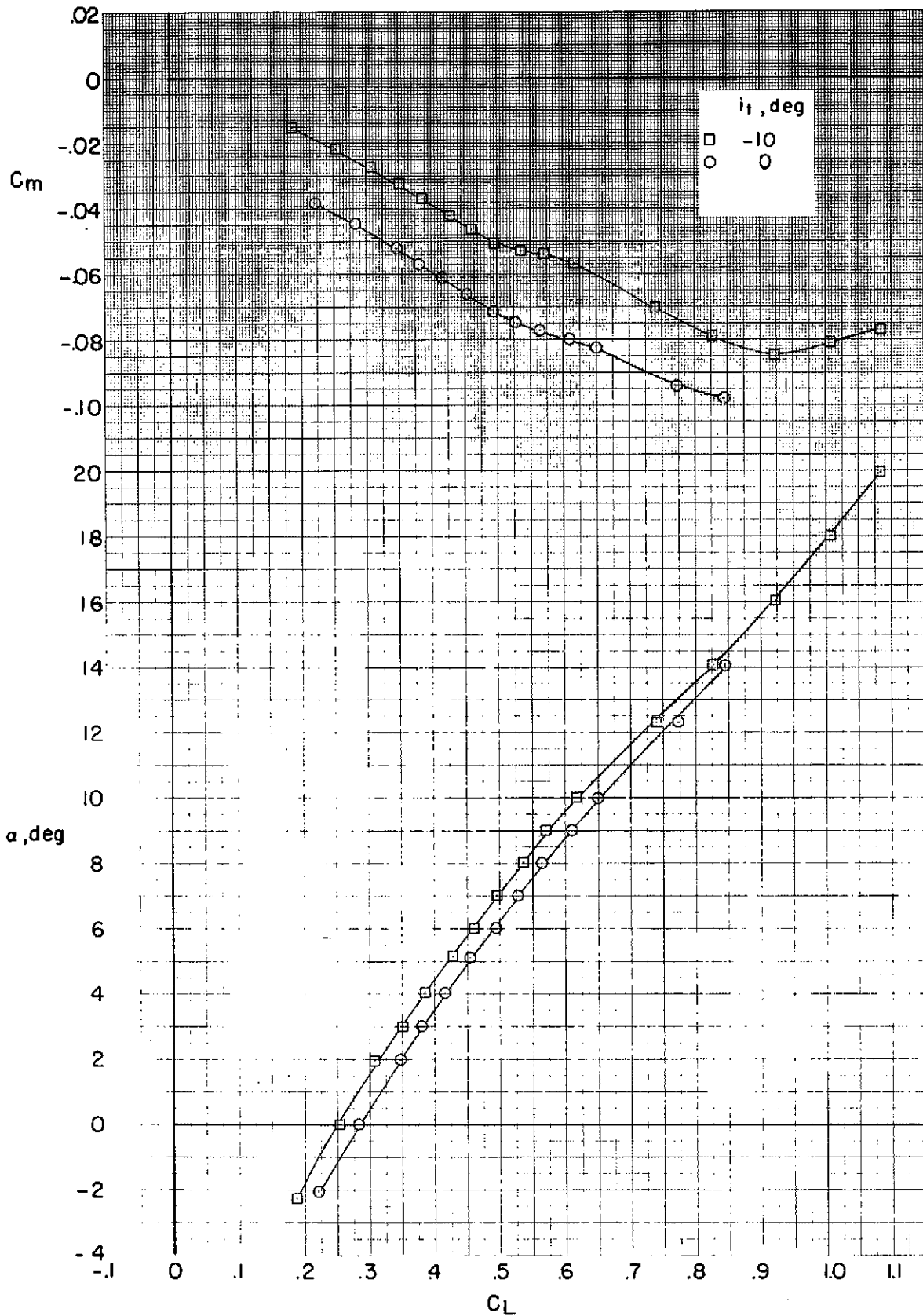


(a) $t_{1,2} = 15^\circ$

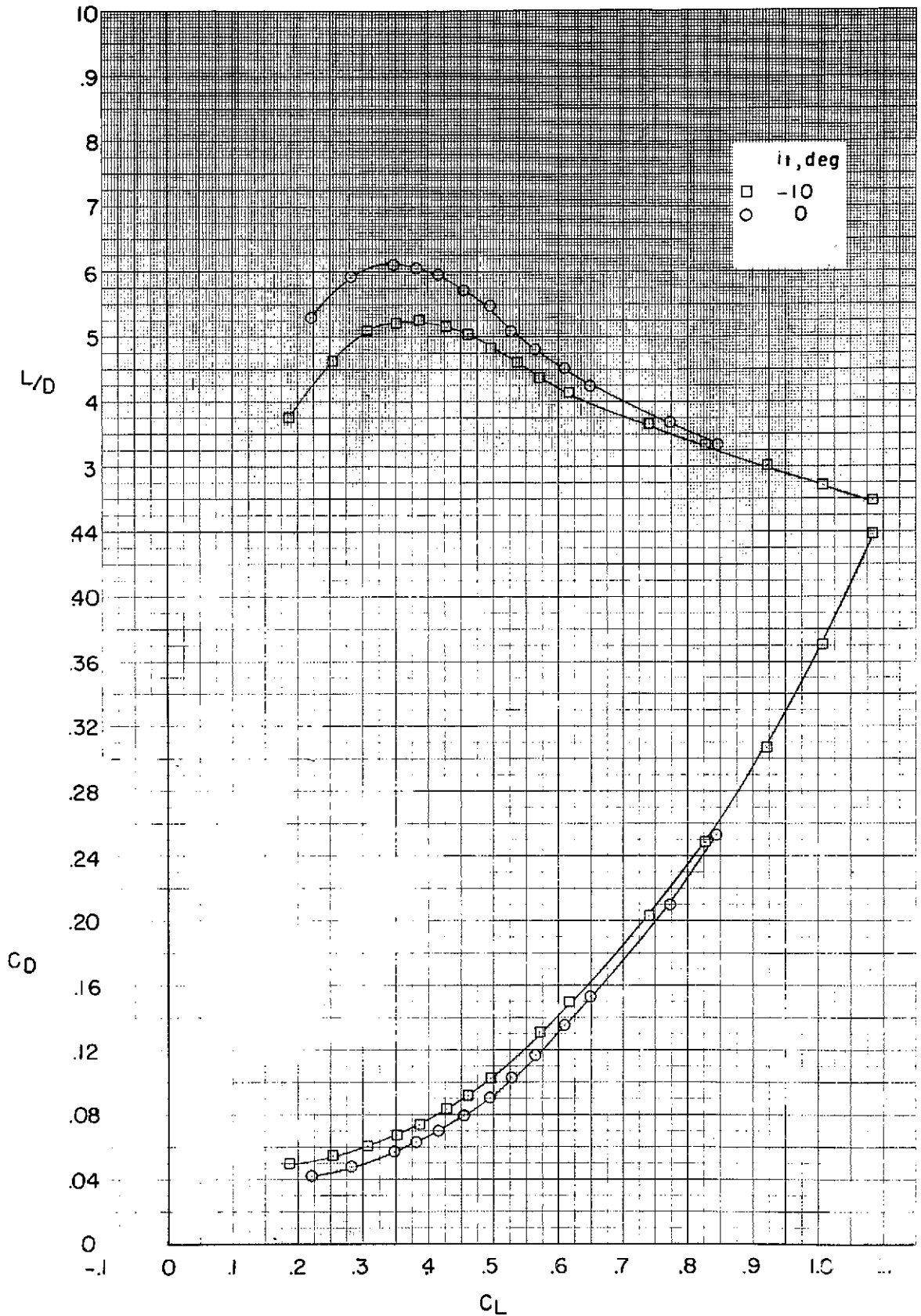
Figure 12.- Effect of horizontal-tail deflection on the longitudinal characteristics.
 $t_3 = 0^\circ$, $t_4 = 5^\circ$, V_{0N} .



(a) Concluded
Figure 12.- Continued.



(b) $t_{1,2} = 30^\circ$
 Figure 12.- Continued.



(b) Concluded
Figure 12.- Concluded.

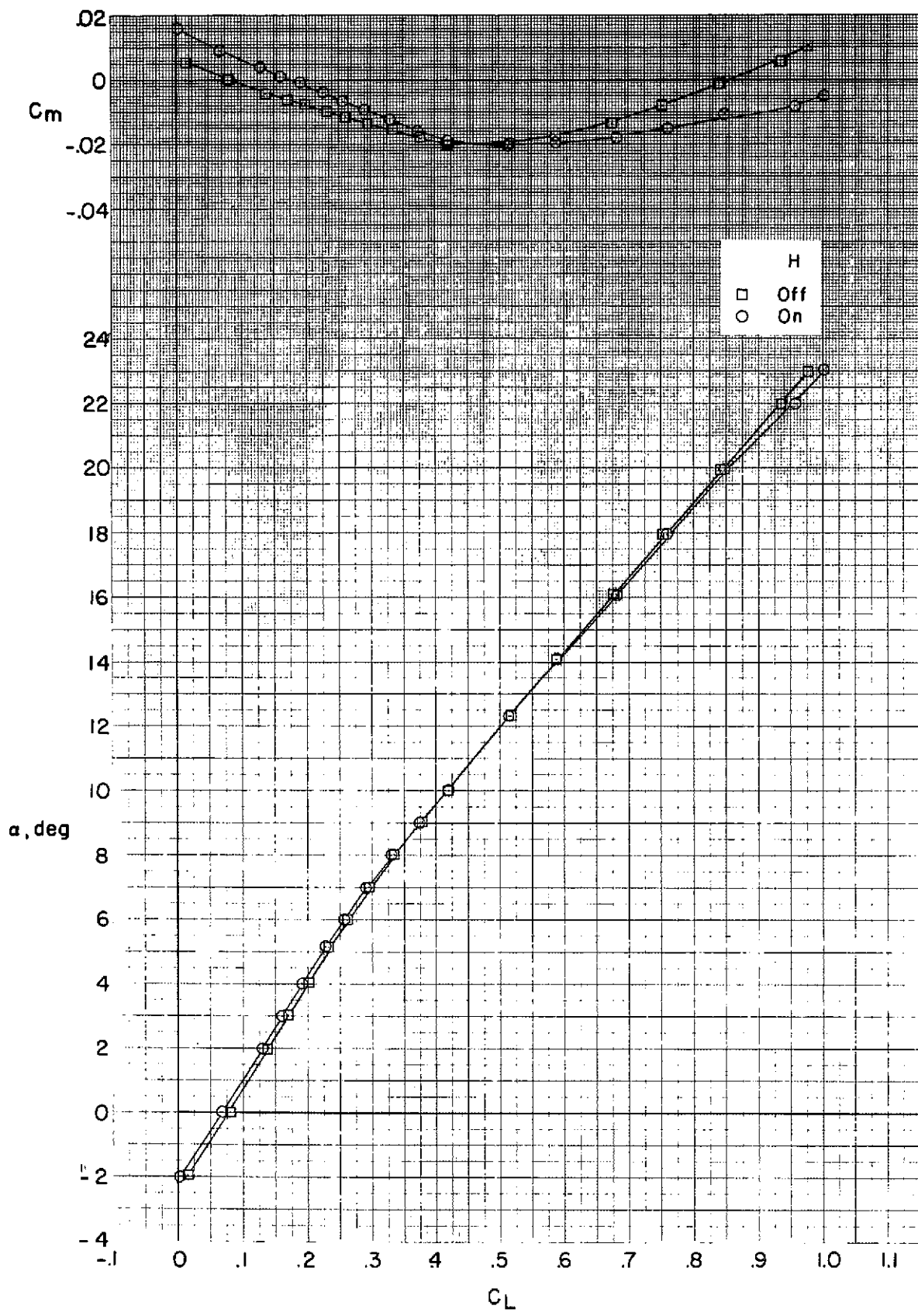


Figure 13.- Effect of the horizontal tail on the longitudinal characteristics.
 $t_{1,2,3} = 0^\circ$, $t_4 = 5^\circ$, V_{0M}

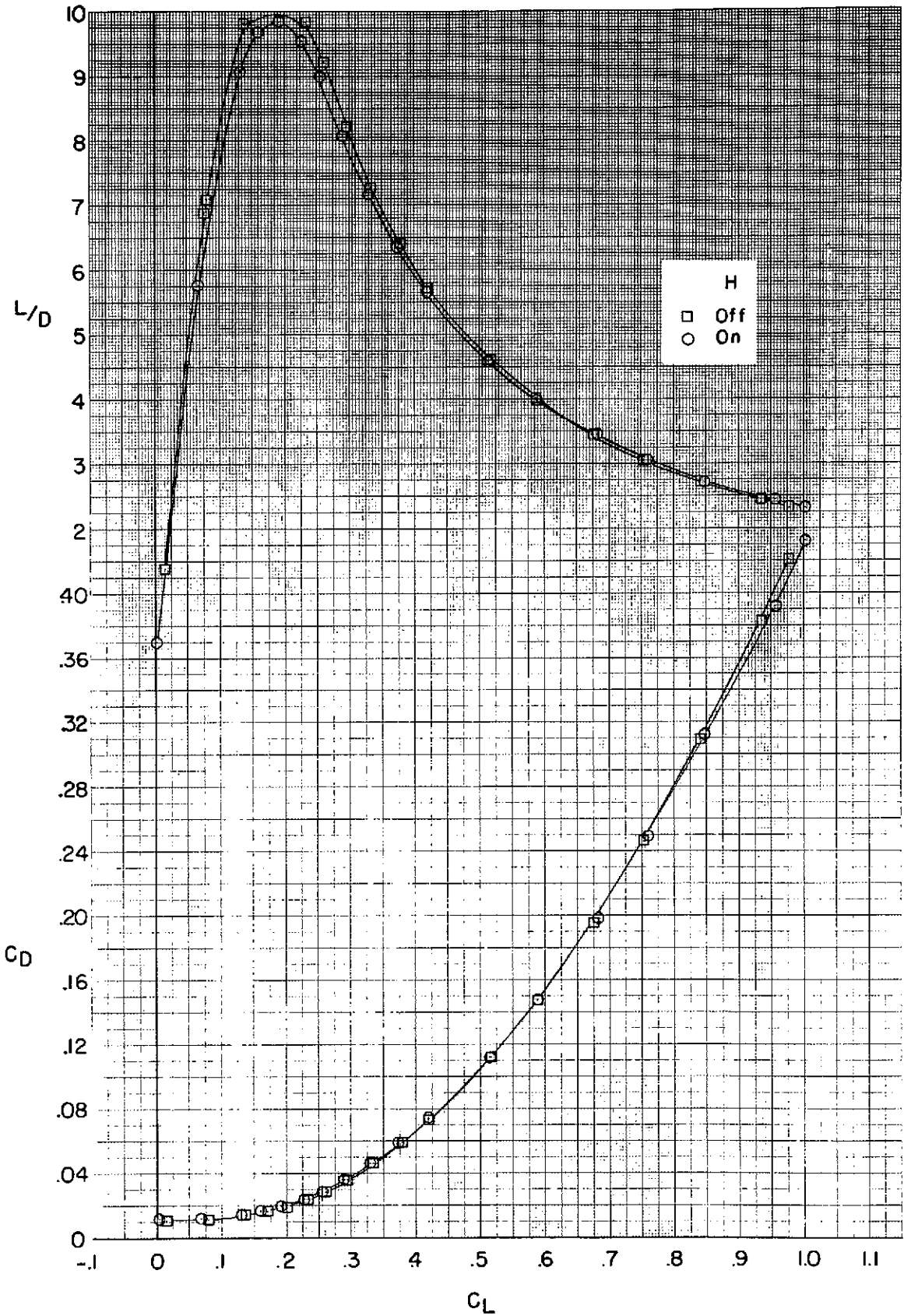


Figure 13. - Concluded.

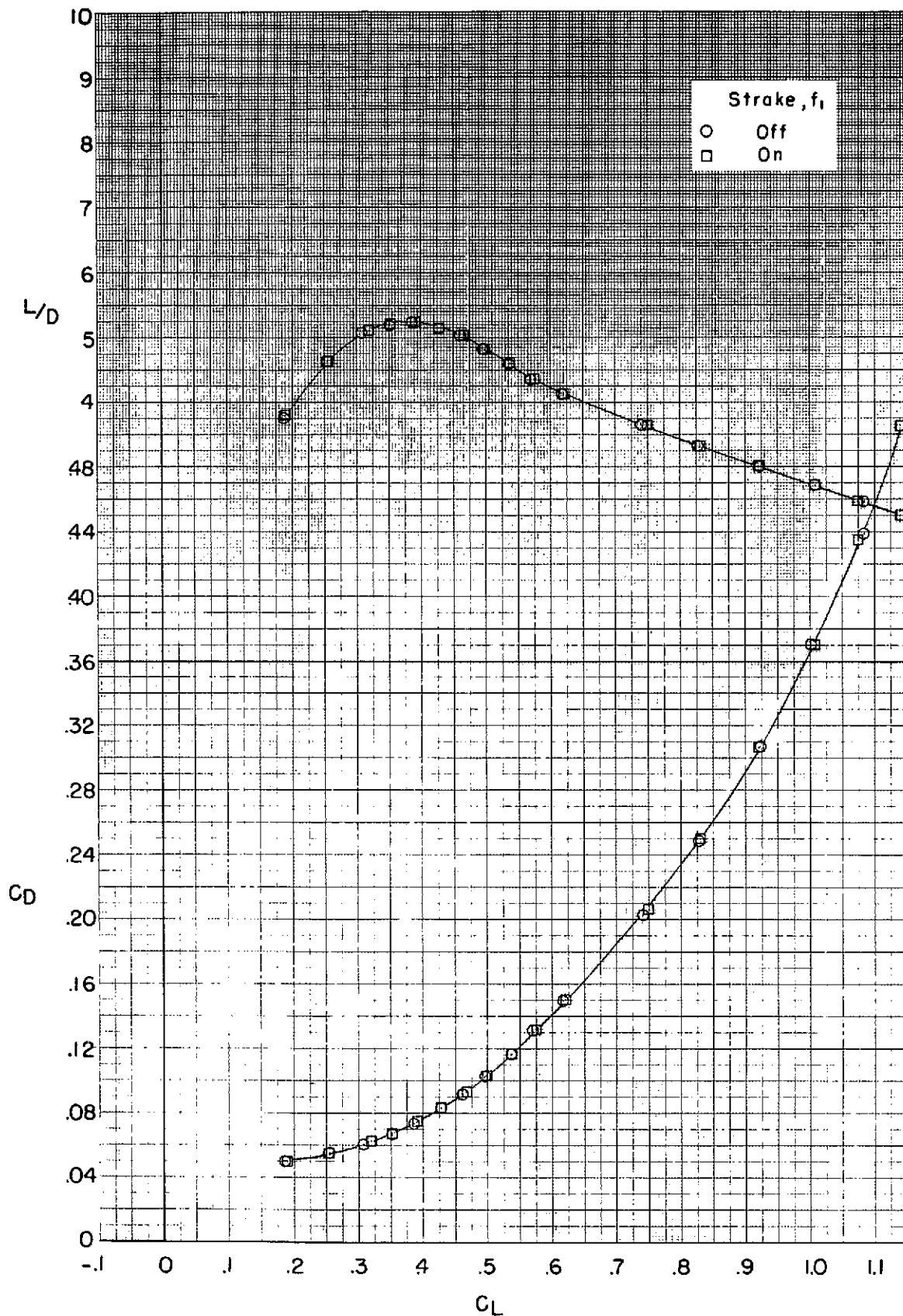


Figure 14.- Effect of the strake on the longitudinal characteristics.
 $t_{1,2} = 30^\circ$, $t_3 = 0^\circ$, $t_4 = 5^\circ$, $t_5 = -10^\circ$, V_{0n}

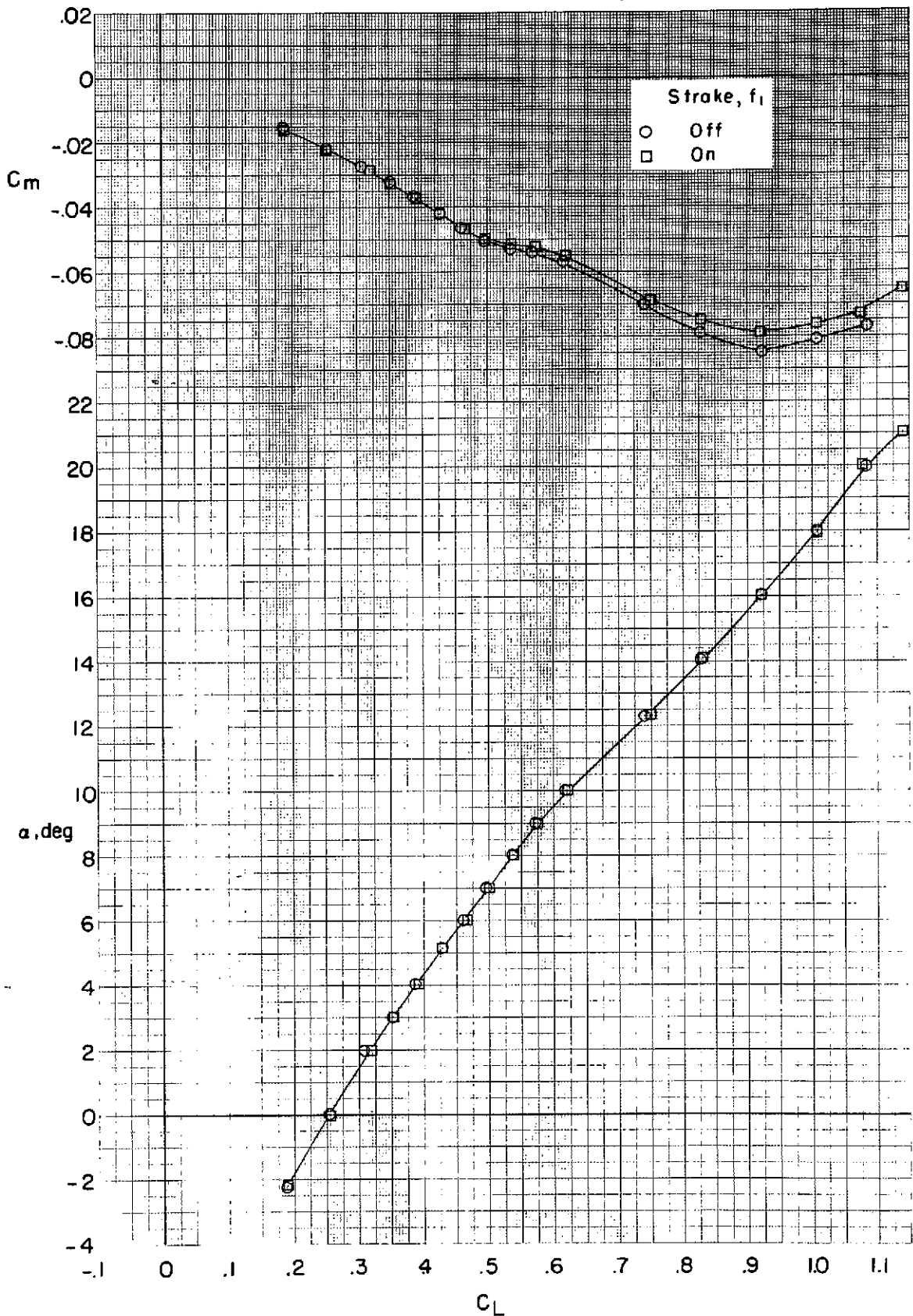


Figure 14.- Concluded.

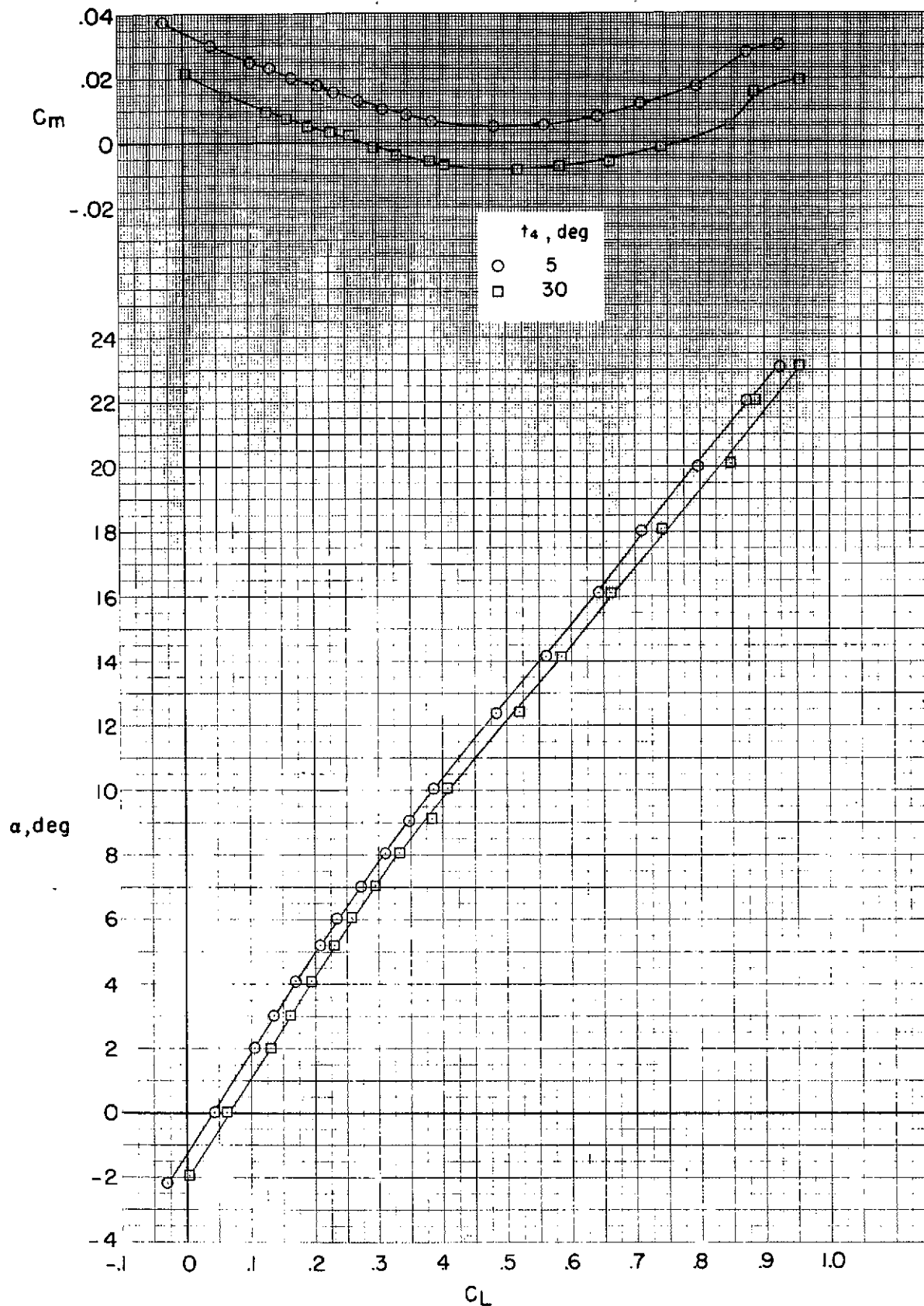


Figure 15.- Effect of trailing-edge flap deflection, t_4 , on the longitudinal characteristics. $t_{1,2} = 0^\circ$, $t_3 = 0^\circ$, $V_{off} \cdot \beta = 5$.

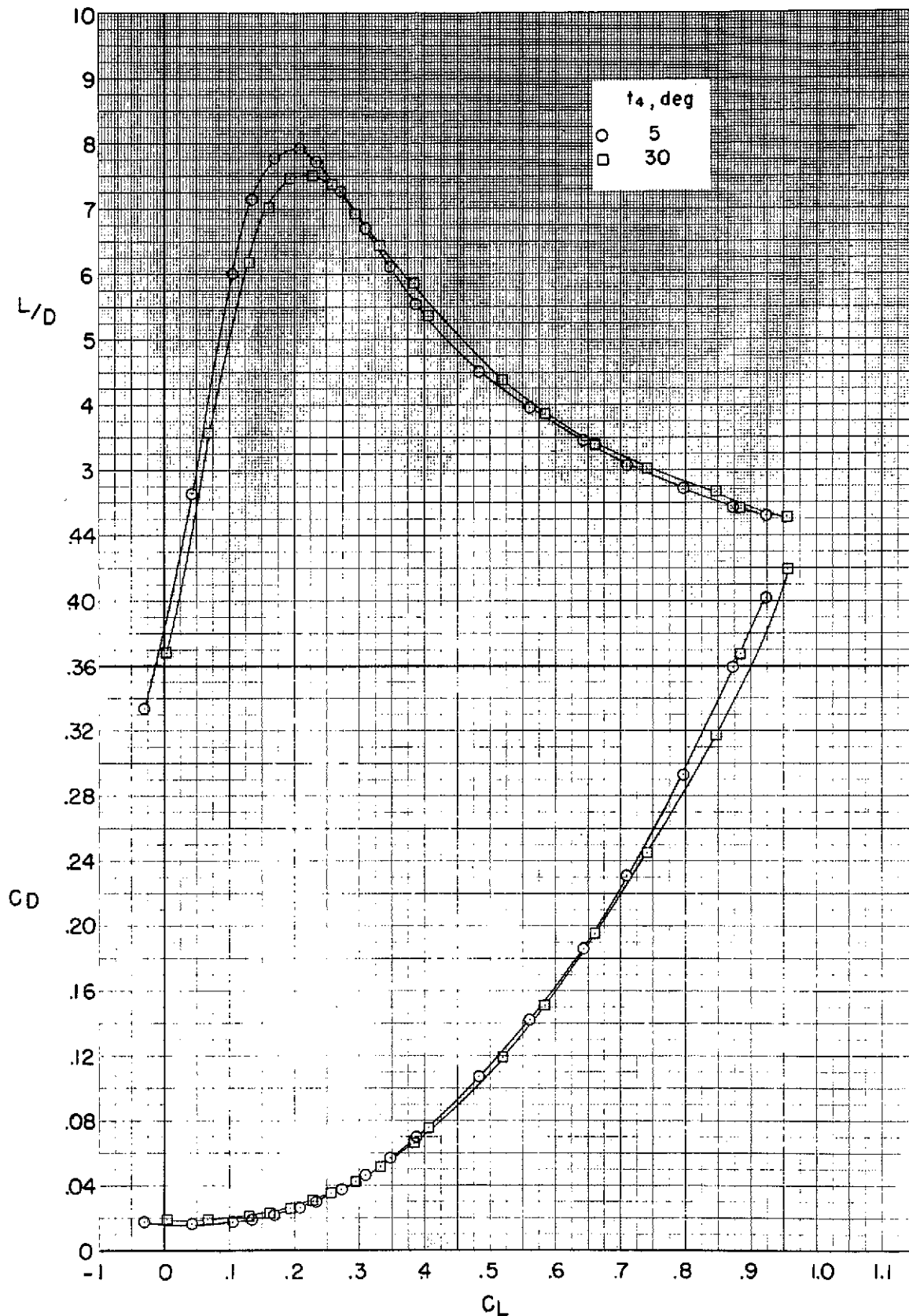


Figure 15. - Concluded.